Walnut shell based adsorbents: A review study on preparation, mechanism, and application

Hania Albatrni, Hazim Qiblawey, Mohammed J. Al-Marri

Journal of Water Process Engineering 45 (2022) 102527

Contents lists available at ScienceDirect

Journal of Water Process Engineering

journal homepage: www.elsevier.com/locate/jwpe

Walnut shell based adsorbents: A review study on preparation, mechanism, and application

Hania Albatrni, Hazim Qiblawey *, Mohammed J. Al-Marri

Department of Chemical Engineering, College of Engineering, Qatar University, P. O. Box 2713, Doha, Qatar

ARTICLE INFO

Keywords:
Walnut shell
Adsorption
Waste minimization
Wastewater
Agricultural wastes

ABSTRACT

Agricultural-based adsorbents have received an upsurge of interest in the water treatment industry especially in the area of adsorption. They have been widely investigated as the next generation adsorbents due to their unique physio-chemical properties and high affinity towards a wide variety of constituents ranging from organic compounds to heavy metal ions. In addition, agricultural-based adsorbents are now a cheaper and sustainable option as opposed to non-renewable and expensive adsorbents originating from coal, polymers, and petroleum residues. Among different agriculture wastes available, walnut shells exhibit great potential as activated carbon precursor. They have outstanding chemical stability, high surface area and low ash content. In this review, walnut shell-based adsorbents have been assessed in terms of their activation methods and preparation. Furthermore, adsorbents' resulting characteristics and factors influencing the adsorption capacity have been summarized and thoroughly analyzed. It has been determined that the adsorption efficiency is heavily associated with the characteristics of the adsorbent including pore diameter, surface area, surface functional groups and the nature of the background solution including pH, temperature and ionic strength. This review identifies different activation methods reported in the literature including chemical and physical activation and chemical impregnation and functionalization. The literature survey also entails a comprehensive discussion involving types of mechanisms and factors controlling adsorption behaviors towards targeted contaminants. Moreover, a detailed analysis of adsorption isotherms and kinetics involved in the adsorption process is also included. Finally, this review mentions future research needs and challenges of adsorption by walnut shell-based adsorbents.

1. Introduction

An economically feasible process of a large-scale production of activated carbon (AC) from low-cost precursors is primitively based on the abundance and availability of waste and by-products. Commonly utilized feedstock for the production of AC includes coal, wood, peat, polymers and petroleum residues all of which are non-renewable and highly expensive [1,2]. As a result, many research works are headed towards the production of AC from sustainable alternatives such as agricultural waste including rice husk, corn straw, sludge, and nuts. Among different agricultural-based adsorbents, the chemical composition of Walnut Shell (WS) exhibits great potential as a sustainable source of AC for the removal of target contaminants from aqueous solutions. Walnuts are produced from *Juglans regia* L, commonly known as the walnut tree, and it is a native plant in central Asia spreading through Europe, western China, Iran and Afghanistan. Walnut production is the second largest nut-production after almond nuts with a production over 3.7 million tons globally in 2019 [3]. The largest producer is China with

Abbreviations: AC, Activated carbon; AR 18, Acid red dye 18; AY, Alizarin yellow; BB, Brilliant blue; BET, Brunauer-Emmet-Teller; BG, Brilliant green; BJH, Barret Joyner and Halenda; BR, Brilliant red; C, Cephalexine; CA, Capric acid; CR, Congo red; DA, Diazinon; DEA, Demthylamino ethyl azide; F, Fluoxetine; FTIR, Fourier transform infrared; HA, Humic acid; IR, Impregnation ratio; LA, Lauric acid; LN-WB, La(OH)3 nanorod/WS biochar composite; M, Methanol; MB, Methylene blue; MG, Malachite green; ML, Metronidazole; MO, Methyl orange; MR, Methyl red; MV, Methyl violet; MWAC, Modified WS activated carbon; MyB, Methyl blue; N, Naphthalene; NA, Nicotinic acid; OA, Oleic acid; P, Phenol; PA, Palmitic acid; PANI@WNS, Polyaniline WS; PD, Pore diameter; PN, Phenanthrene; PZC, Point zero charge; RB, Rhodamine B; RB 19, Reactive blue 19; RB 5, Reactive black 5; S, Sulfamethozale; SEM, Scanning electron microscopy; T, Tetracycline; TCF, Trichlorophenol; TETA, Triethylene tetramine; TG, Gravimetric analyzer; V_m, Micropore volume; V_t, Total pore volume; WS, Walnut Shell; XRD, X-ray diffraction; ZPA, Zeta potential analysis.

* Corresponding author.
E-mail address: hazim@qu.edu.qa (H. Qiblawey).

https://doi.org/10.1016/j.jwpe.2021.102527
Received 10 October 2021; Received in revised form 13 December 2021; Accepted 15 December 2021
Available online 29 December 2021

an annual production of 1.06 million tons of walnuts followed by USA with a production around 600 tons and Iran with a production close to 405 tons [4]. WS make up 67% of the total weight of the fruit and they typically consist of cellulose, hemicellulose and lignin [5,6]. These agricultural wastes are normally discarded with no further use post cultivation or incinerated for heating purposes.

WS have proved effective in several applications including particle board industry. They have been used as raw material for wood-based particleboard, which has been examined by Pirayesh et al. [7]. Embedding WS not only immensely improved the water resistance of the panels, it also minimized the usage of virgin wood materials in turn, saving natural resources. During the industrial revolution, the use of WS was initiated in more pressing applications such as the production of charcoal and Activated Carbon (AC) through pyrolysis [8]. Schroder et al. experimented with different sources of biomass including WS, rice, wheat, straw, olive stones, pistachio shells, beech, and hard coal [8]. Pyrolysis was performed at a temperature range of 500–600 °C at a heating rate of 10 K/min. Furthermore, the biomass was activated through steam activation at temperatures between 800 and 900 °C. The results demonstrated that nut shells provide larger active surfaces than that of straw-base materials signifying the presence of high amounts of carbon in nut shells and high ash content in straw-base materials. As of late, WS are employed as precursors in the preparation of AC for the removal of hazardous materials from industrial wastewaters [9–13]. Hazardous contaminants commonly targeted in the experimental field include heavy metal ions and synthetic dyes. However, AC is the first adsorbent to be recognized and utilized in the industry for the removal of oil. Limited studies have been reported on the removal of oils using walnut-based AC in the literature. Srinivasan et al. reported that WS have a high affinity towards oils with uptake capacities ranging from 0.56 to 0.84 g/g [14]. However, many reported the successful utilization of WS in the removal of organic compounds such as phenols, methanol, and polyaromatic compounds [15–17]. Generally, nutshells have also been employed in its natural state without activation or further modification. Dias et al. examined five different nutshells including walnuts, hazelnuts, peanuts, pistachio and almonds shells for the removal of heavy metal ions [18]. High efficiencies of 90% have been reported proving their ability in remediation of contaminated waters. Moreover, WS have also used in enhanced removal of oil from oilfield wastewaters [19].

Employing raw biomass without further modification may not yield desired results due to their limited functionalities. For example, biomass prior to activation has relatively low pore properties inhibiting its ability to reach full capacity in the adsorption process. Thus, there is an increasingly growing research interest in identifying new methods to improve chemical or physical properties of biochar. Pyrolysis temperature is one of many factors that can improve the yield of the resulting biochar. Demirbas et al. studied the effect of temperature on pyrolysis products from four nut shells including hazelnut, walnut, almond and sunflower in a range of temperature between 500 and 1200 K in a cylindrical batch reactor [20]. The results show that to maximize char yield, a low temperature and heating rate is recommended. Increasing temperatures would only decrease char production. Chemical and physical activation also play major roles in the enhancement of properties of WS-based adsorbents. Qiongfen et al. prepared WS AC by chemical activation where the resulting surface area was 1636 m^2/g competing with commercially available ones [17].

Walnut-based adsorbents have been explored as the next generation adsorbents for the removal of emerging contaminants, compounds that have been recently discovered including pharmaceutical drugs, personal care products, veterinary products, herbicides, food additives engineered nanomaterials and industrial compounds. These contaminants have long existed in the environment; however, only recently their existence and effects are being identified. Latest studies show that WS have high affinity towards these contaminants [9,12,13,21,22].

The adsorption efficiency of target contaminants by WS is maneuvered by several factors related to the type of the activation process of WS that is responsible for the creation of the pore structure and surface chemistry, nature of the target compounds, in addition to the chemistry of the water to be treated. Thus, the aim of this review paper is to conduct a comprehensive review on peer-reviewed articles on WS-based adsorbents for the treatment of water or wastewaters. The objectives are divided into two subcategories. The first goal is to discuss the resulting properties of walnut shell-based adsorbents with respect to different methods of enhancement including physical activation, chemical activation and chemical impregnation. The second goal is to examine and study the mechanisms and factors controlling the adsorption process of target contaminants onto WS-based adsorbent. For the purpose of this review paper, target contaminants to be focused on can be broadly classified into heavy metal ions and organic compounds with a major focus on organic dyes.

2. Walnut shell chemical composition

The lignocellulosic compounds account around 70% of the total biomass among different types of plant or wood biomasses [23]. The main constituents of WS are very similar to that of wood biomass which include lignin, cellulose, hemicellulose and tannins that can be extracted and utilized to create other chemicals and materials [24]. The elucidation of chemical components of WS is extremely difficult due to the presence of highly crosslinked-polymeric structures in the shell. Since WS are used in a widespread of applications, it is crucial to be able to identify its chemical components. It has been reported that the approximate percentage chemical composition of WS consists of 50.3% lignin, 22.4% hemicellulose, 23.9% cellulose and 3.4% ash [25]. However, the percentage of each component can slightly vary depending on the source of the walnut, plant genetics, the environment where the plant was grown and processing conditions of the fruit. Fig. 1 represents chemical composition of WS reported by different researchers in the literature. Reported ash and extracts percentages from different studies are similar with slight variations. The chemical composition of WS are also presented in Table S1 in the supplementary data file.

Queiros et al. characterized the shells of three different nuts in terms of their chemical and extract composition [4]. All three nuts were produced in Portugal and collected from different local supermarkets. It was noted that WS contained 0.7% ash, 10.6% total extractives, 29.9% lignin and 49.7% polysaccharides. Detailed chemical compounds present in WS are presented in Tables 1 and 2. WS composition differs from other nut shells in terms of hemicellulose where the contents are mainly Xylans that are highly functionalized with acetyl groups and galacturonic

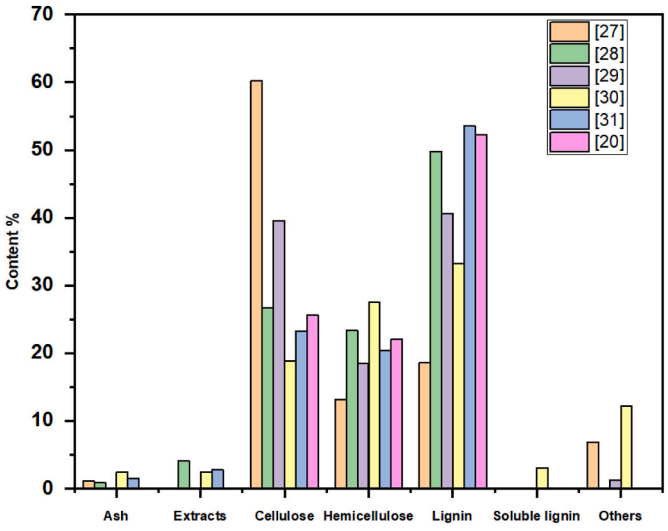

Fig. 1. Percent content of chemicals in WS reported in the literature.

Table 1
Chemical composition in % total dry mass of WS [4].

Total extractives	10.6
Ash	0.7
Total lignin	
Klason lignin	29.3
Soluble lignin	0.6
Polysaccharides	
Rhamnose	0.6
Arabinose	0.7
Galactose	1.4
Glucose	21.7
Xylose	19.3
Galacturonic acid	2.6
Glucuronic acid	0.1
Acetyl	3.3

acid. Overall, WS can be characterized with high lignification (SG lignin), moderate content of polar extractives and low content of minerals [4]. From Table 2, it is noted that WS contain substantial amounts of calcium and potassium including magnesium and iron. Demirbas et al. studied the effect of temperature on pyrolysis products from four different types of biomasses [20]. Biomasses experimented in the study originate from hazelnut, walnut, almond and sunflower. Zhai et al. reported results of GC–MS analysis of pyroligneous acids extracted from WS [26]. Main components included dominating compounds organic acids and phenols in addition to ketones, aldehydes, alcohols, esters, benzene and its derivatives, and sugar and its derivatives. Similar results of WS pyroligneous acid have also been reported by Jahanban-Esfahlan et al. [24].

Another study reported the extraction and characterization of lignin compounds present in WS using GC–MS and H NMR techniques [27]. Major compounds identified in this study include Guaiacol, 4-methylguaiacol, 4-ethylguaiacol, 4-propylguaiacol, syringol, 4-methylsyringol, 4-ethylsyringol and 4-propylsyringol.

3. Characterization of walnut shell

WS-based adsorbents need to be thoroughly characterized before and after adsorption in order to have an insight into their distinctive properties and be able to identify the type of adsorption mechanism that takes place at the surface of the adsorbent. Adsorption of contaminants onto the adsorbent is a consequence of both surface chemistry and adsorbent morphology. WS-based adsorbents have been the subject of numerous adsorption studies especially for the removal of heavy metal ions. Furthermore, they have been extensively tested for the removal of organic compounds where dye methylene blue has been commonly utilized as a model representation. Crucial chemical properties to be characterized include surface chemistry, charge, polarity, and purity of the final effluent. The morphology of the adsorbent includes specific surface area, total pore volume, pore size distribution, texture, and structural geometry. Principle techniques responsible for characterization that are commonly utilized according to the literature include Brunauer-Emmett-Teller (BET), Scanning electron microscopy (SEM), X-ray diffraction (XRD), Fourier transform infrared (FTIR), N_2 adsorption-desorption isotherms at 77 K and zeta potential analysis.

Considering that WS based adsorbents are activated and functionalized using different techniques and functional groups it is highly likely that the specific surface area, pore volume and average pore size will vary significantly. Most common characteristics reported in the literature are tabulated and presented in Table 3. The BET technique is used to identify the specific surface area and the total pore volume can be calculated from the adsorbed volume of nitrogen near the saturation point P/P0. The average pore size distribution is commonly obtained according to the method derived from Barret, Joyner, and Halenda (BJH) [28]. Ashrafi et al. removed brilliant green and congo red dyes from aqueous solution using WS modified with NaOH [29]. The modified WS adsorbent showed in increase in the specific surface area by a factor of 2.3. Zhou et al. used commercial activated carbon derived from WS for the removal of diazinon pesticide from aqueous solutions [30]. The activated carbon was further modified with phosphoric acid to increase adsorption efficiency [30]. The morphology of the adsorbent largely improved with an increase in specific surface area from 1076 to 1434 m^2/g and a decrease in average pore diameter and total pore volume from 3.23 to 2.08 nm and 0.86 to 0.74 m^3/g respectively. Li et al. successfully introduced aspartic acid onto the surface of WS morphically enhancing the characteristics of WS where all three characteristics specific surface area, total pore volume and average pore diameter increased from 1.04 to 2.33 m^2/g, 3.13 to 12.18 m^3/g and 12.09 to 20.92 nm respectively. Zhou et al. also reported an increase in specific surface area and total pore volume post functionalization of WS based

Table 3
Morphological characteristics of raw and modified WS in the literature.

Adsorbent	BET surface area (m^2/g)	Total pore volume (m^3/g) x 10^{-6}	Average pore size nm	Reference
Raw WS chemically activated with phosphoric acid	420.5	–	2.25	[36]
Raw WS was mixed with colloid solution Fe (NO3)3.9H2O and Na2CO3 solution	640.9	0.2954	1.844	[37]
RWS impregnated with $MgCl_2$	25.12	2320	52.31	[38]
Commercial grade WS	614.2	460	3.4	[32]
synthesized using solid sodium hyroxide and aspartic acid	2.33	12,180	20.92	[39]
Fe/Fe3C nanoparticles incorporated onto WS	1779.3	0.9	0.38	[31]
Hydrothermal carbon was produced from WS and chemically activated using nitric acid	84	0.361	4.2	[10]
WS impregnated with 30% phosphoric acid	410.84	0.61	5.92	[40]
WS chemically active with phosphoric acid	1434	0.74	2.08	[30]
NaOH-modified WS	2.095	0.0171	32.64	[29]
WS modified by non-thermal plasma in ultrafine water mist	1.11	–	–	[41]
WS modified with a mixture acetic acid and hydrogen peroxide	1.2	0.16	0.03	[42]
Raw WS	2.41	–	–	[43]
Raw WS	10.16	–	–	[44]
Nanomagnetic WS-rice husk	126.72	8.11	0.418	[45]
Raw WS	934	0.457	–	[45]
Cu-doped WS -based AC	206.6	0.2602	5.038	[46]

Table 2
Mineral composition in mg/Kg dry mass of WS [4].

Na	K	Ca	Mg	P	S	Fe	Cu	Zn	Mn	B	Mo
554	5202	9081	1283	691	791	3095	6.2	18	111	29.7	9.9

adsorbent. However, average pore diameter remained the same [31]. Chunli et al. reported that the porosity of the WS adsorbent massively improved through hydrothermal carbonization from 2 to 84 m^2/g [10]. According to pore size analysis, the average pore size diameter of activated WS is located within the mesopore range [32].

SEM, FTIR and XRD all of which can provide further morphological characteristics of WS. SEM delivers an insight into the structure, shape, and surface of the WS based adsorbent. The addition of functional groups onto the surface of the adsorbent can alter the chemistry of the surface by changing its hydrophobicity and consequently, the additional functional groups can be described using FTIR and XRD [33]. Luo et al. synthesized a $La(OH)_3$/WS composite for the removal of phosphate ions [34]. From the FTIR analysis, it can be observed that $La(OH)_3$ was successfully imbedded onto the surface of activated WS through the additional peaks that appeared in the FTIR spectrum that were assigned to stretching vibrations of O-H and La-OH. According to the XRD analysis WS has no characteristic absorption peaks indicating that WS is an amorphous substance, however, post functionalizing with $La(OH)_3$, the results showed that the phase was hexagonal in shape. The way in which the adsorbent behaves when in contact with aqueous solutions highly depends on its point zero charge, which can be measured using zeta potential analysis. Generally, when the pH of the solution is above point zero charge, the surface tends to be negatively charged. Conversely, when pH of solution is below point zero charge, the surface tends to become positively charged. Depending on target contaminant, whether negatively or positively charged, the surface chemistry can be controlled by altering the pH in order to enhance the adsorption process. Major adsorption mechanism plays a crucial role in such cases where it is dominated by electrostatic interactions between surface functional groups and target contaminant. Ashrafi et al. reported the adsorption mechanism of $Pb2^+$ ions onto modified WS was due to electrostatic interactions between positively charged lead ions and negatively charged functional groups COO^- and OH^- at pH values higher than the pH_{ZPC} [35].

4. Overview of WS based adsorption studies

The majority of WS studies follow the same pattern where the focus of study can be divided into three subdivisions. The first section includes synthesis, functionalization, and characterization of WS; the second area focuses on the adsorption process of organic compounds or heavy metal ions. Lastly, the last area discusses the mechanism of adsorption and modeling of the behavior of contaminants towards the adsorbent. Nonetheless, there still exists a need to fully comprehend the mechanism of adsorption towards WS and what are the major factors that influence the adsorption process. For the purpose of this review paper, 73 papers have been thoroughly examined and peer reviewed. The established time frame for the papers to be selected in this study is between and including 2016 and 2021.

Target contaminants that have been studied in selected review papers can be broadly classified into two groups organic compounds and inorganic compounds. Most of the organic compounds studied are synthetic dyes with a major focus on methylene blue as a model for organic compounds. A bubble plot has been developed on Excel depicting all organic compounds utilized in this research and presented in Fig. 2. In total, 29 different compounds have been examined 17 of which are synthetic dyes. The second group of organic compounds focused on belong to emerging contaminants such as phenanthrene, cephalexine and Sulfamethozale antibiotics [12,22]. Polycyclic aromatic compounds such as naphthalene have also been studied [16,32]. From Fig. 2, it is deduced that the molecular weight of most of the organic compounds studied fall within the range of 100–400 g/mol.

Heavy metal ions have also been a major focus in WS studies where the most studied element is Pb. Fig. 3 shows the number of studies that underwent the adsorption of heavy metals in total and it is evident that Pb is in the lead with 7 papers followed by Cu with 5 reported studies. These studies are also presented in Table S3 in the supplementary data file. To further enhance the uptake capacity, WS are further modified prior to experimental tests and as such, a comparison between two experimental tests with two different modification techniques is difficile. Of the selected 73 papers, 15 utilized WS as is with no further modification and a comparison between these tests is more practical. A more detailed analysis is provided in the next sections. Supplementary data regarding those studies are presented in Table S2 in the supplementary data file.

5. WS preparation modification

Raw materials have limited ability to adsorb various contaminants, especially in the field of water treatment. Thus, in order to enhance the adsorption uptake or increase the affinity of target contaminant towards the adsorbent, numerous measures have been employed to alter

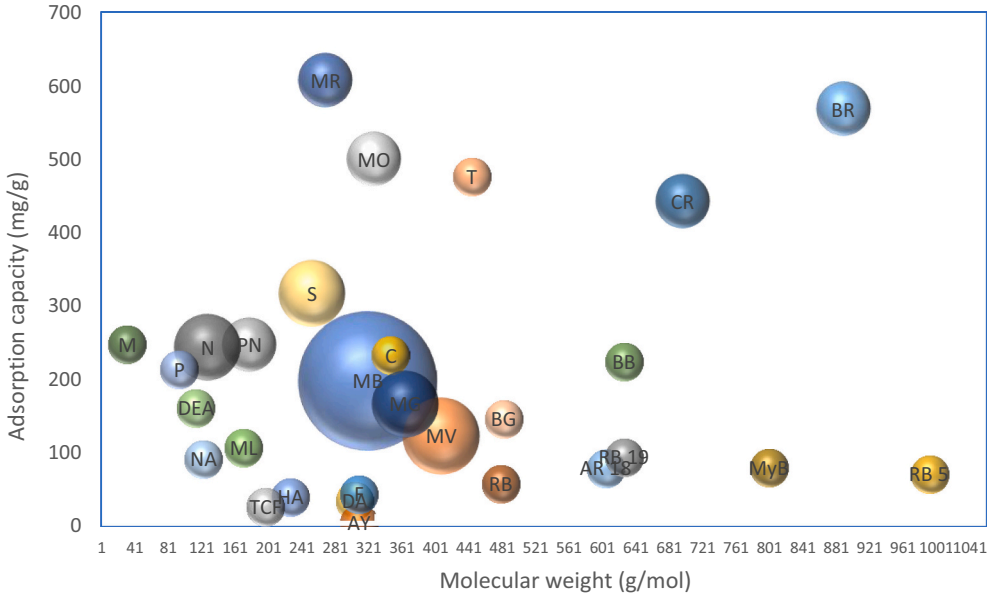

Fig. 2. Bubble plot of the literature review detailing adsorption studies of organic compounds during the period 2016 and 2021.

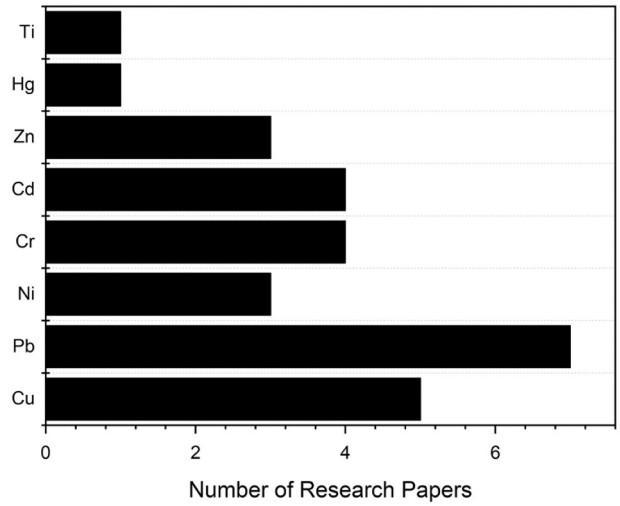

Fig. 3. Bar chart of the literature review detailing adsorption studies of heavy metal ions during the period 2016 and 2021.

physiochemical properties of WS. Physical and chemical activation does not only improve physical/chemical properties of the adsorbent, but also expands the application of bio-adsorbents to several fields outside the area of water treatment. The enhancement can be observed in the increase of functional groups, specific surface area and pore volume. Generally, the modification of WS adsorbent normally undergoes a series of steps starting from the first stage of preparation in which raw WS is crushed to the desired size followed by a washing process with distilled water after which the material is dried at a temperature of 105 °C overnight or for 24 h. The next process is the activation process where chemical or physical activation is normally utilized. Then, the carbonization procedure is performed during pyrolysis, it can also be referred to as thermal treatment, at an inert atmosphere where an inert gas, such as nitrogen or argon, flows at a predetermined flow rate and temperature. In some cases, pyrolysis is performed prior to the activation step. Finally, the series of modifications ends with the functionalization process. A detailed explanation of the activation and functionalization steps are provided in the sections to follow. Fig. 4 provides a general idea of different methods of modification of WS available in the literature. Most of the research works is performed either through chemical activation or chemical modification/impregnation. In order to follow a path of less chemical usage and an environmentally friendly approach, researchers are employing raw WS without any type of modification. Lastly, physical activation is the least employed method of modification.

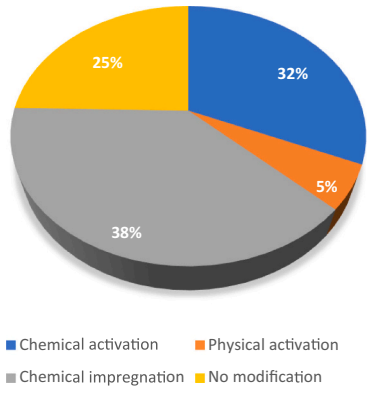

Fig. 4. Different methods of WS modification.

5.1. Physical activation

Physical activation is defined as the partial gasification of biomass using single or combination of gases such as steam, air, or carbon dioxide at predetermined conditions of temperature and gas flow rate [47]. It is a two-step process consisting of the carbonization step in a neutral atmosphere and then in the atmospheric oxidizing gases with increasing temperatures ranging from 800 to 1000 °C [48]. It has been reported that carbon dioxide yields a greater uniformity of pore structure and that the activation can be easily manipulated at temperatures around 800 °C as activation is a slow reaction rate process [49]. Physical activation is performed before or after the pyrolysis step; however, in most cases it is performed after pyrolysis to further enhance the porosity of the biochar. This method is an inexpensive method to yield activated carbon of high porosity and an environmentally friendly approach considering that it does not require the use of chemicals [50]. However, it is a time consuming and an energy intensive method [50]. Pazouki et al. synthesized by co-precipitation magnetic nanoparticle supported on AC from WS. Physical activation was performed using water vapor at 800 °C [51]. Physical activation increased the oxidation resistance of supported magnetic particles.

A few studies have undergone the method of physical activation to activate WS and are listed in Table 4. Derdour et al. prepared AC by physical activation with water vapor at different temperature to investigate the effect of the temperature on the char structure [52]. Contaminants removal increased with increasing activation temperature. The optimum activation temperature reached is 900 °C after which a decrease in adsorption capacity was observed. Roman et al. experimented physical activation with air and carbon dioxide for the removal of Fluoxetine and nicotinic acid [21]. It was stated that the adsorption process is highly influenced by surface chemistry rather than the porous structure of the material. Maximum adsorption capacity reached for the removal of fluoxetine with air as the activating agent, while for the removal of nicotinic acid, the maximum adsorption capacity was reached with carbon dioxide activation. Carbon dioxide activation enhances surface basicity of the AC delocalizing basal plane electrons that provide a stronger Π-Π interactions between the AC and nicotinic acid's aromatic rings.

5.2. Chemical activation

Chemical activation, or wet oxidation, involves the usage of chemicals at high temperatures [50,53]. The starting material is usually a source of biomass that is a cellulose-based material and is termed as an organic precursor. There are various chemical agents used in the literature including phosphoric acid, zinc chloride, potassium hydroxide, sodium hydroxide, potassium carbonate and other emerging chemical activating agents. Chemical activation is a two-step process. The first step is the saturation of the raw material with oxidizing and highly dehydrating chemicals. This step can be carried out via two methods which are the impregnation and physical mixing methods [53]. Impregnation involves the initial mixing of the precursor and the chemical activating agent in appropriate volumes. This procedure is often performed in the presence of hydroxide agents and heated to a desired temperature until a brown-colored sludge is developed after which the sample is then filtered and dried. In physical mixing, precursors are directly mixed with the activating agent in solid state in a furnace where activation occurs at temperatures ranging from 400 to 900 °C. Carbonization or pyrolysis is the second step of the chemical activation process, in some cases, it is performed prior to the activation step. Finally, the last step in the chemical activation procedure is the washing step. This step is crucial as it removes chemical residues that occupy the porosity of the resulting AC [54]. Hence, to further develop AC's porosity, washing must be performed. It is usually carried using acids or alkali agents depending on the chemical activator used followed by rinsing with water.

Table 4
WS adsorption studies underwent physical activation.

Technique used	Outcome of activation	Contaminant	Effect on adsorption capacity	Reference
Water vapor at 800 °C		Hg	Increased the oxidation resistance of supported magnetic particles	[51]
Two fluids: air at 250 °C and flow rate of 100 mL/min for 30 min and CO_2 at 850 °C for 30 min at 40 mL/min	Activated carbon produced from CO_2 activation are basic and have a net positive charge	Fluoxetine and nicotinic acid	Activation with CO_2 showed faster kinetics and higher affinity at lower concentrations Activation with air showed slower kinetics	[21]
Combination of water/N_2 for 2 h at rate of 10 °C/min at different temperatures (700, 800, 900 and 1000 °C)	Optimum activation temperature reached at 900 °C	Cr(VI)	Marginal increase in Aadsorption capacity increased from 9.23 to 10.11 mg/g	[52]

AC through chemical activation yields a more porous structure than AC formed through the physical activation process [55]. Chemical agents utilized in the chemical activation process are dehydrating agents, thus, they have the ability to alter pyrolytic decomposition by preventing the formation of tar, increasing activated carbon content and in turn, developing a highly porous structure of carbon material [56]. Moreover, surface area is enhanced through the penetration of chemical activating agents into the carbon structure forming micropores in the process [55]. It is more economical as it requires lower activation temperatures and it is less time consuming. In contrast to physical activation processes that are energy intensive and time consuming. However, the disadvantage of employing chemical activation is the generation of chemical waste during the washing process to eliminate chemical residues post activation process.

Chemical activation can either be performed on carbonized carbon or on WS or other source of biomass at its raw or pre-carbonized state. Among chemical activators, H_3PO_4 and $ZnCl_2$ can be performed on raw materials. Cellulose is known to be resistant to hydrolysis of acid thus allowing lignocellulosic materials to react with H_3PO_4 [53]. A number of studies have performed chemical activation on WS using H_3PO_4 [30,36,40,57–60]. Zheng et al. reported that activating with H_3PO_4 results in a mesoporous surface on AC [40]. SEM images of a fresh AC exhibited an irregular clear pore structure. From the XPS survey spectrum, P was detected due to the impregnation process. Major peaks from the FTIR spectrum demonstrated the presence of aromatic rings, carboxyl groups, alkoxy groups, hydroxyl groups all of which played a major role in the adsorption process through the Π-Π interactions and interactions between phenanthrene (studied contaminant) and oxygen containing functional groups.

H_3PO_4 combines chemically within the lignocellulosic structures. It has been proposed that there exists a link between porosity enhancement and the formation of cross-linked structures in the form of phosphate esters when H_3PO_4 is used. Bayat et al. reported the presence of a peak from the FITR analysis that belongs to P=OOH or the P-O-C linkage [30]. Moreover, according to the FTIR analysis, H_3PO_4 promotes pyrolytic decomposition of the starting material leading to the elimination of some functional groups creating a more grid structure in the process. Ojo et al. conveyed that H_3PO_4 modification improved the surface functional groups of WS leading to broader functional groups including carbonyl and hydroxyl groups that are key players in the adsorption process [58]. A study conducted by Donald et al. revealed that H_3PO_4 requires low activation energy usually ranging from 400 to 500 °C [61]. Activation using H_3PO_4 occurs through the formation of cross-linked phosphate esters that reach their thermal stability at temperatures between 400 and 500 °C. Consequently, activation at higher temperatures will result in the breakdown of these links causing contraction and hence, reduction in porosity development. Alimohammadi et al. investigated the removal of reactive red dye 198 using both batch isotherms and fixed bed columns [57]. Two chemical activating agents were investigated in the study KOH and H_3PO_4. The type of activating agent and impregnation ratio heavily impacted the shape of N_2 adsorption/desorption isotherms. At high H3PO4 impregnation ratios, the BET surface area and mesoporosity increased drastically. A list of studies that employed H_3PO_4 for activation of WS are presented in Table 5. As can be seen, almost all research studies employed an activation temperature between 400 and 500 °C.

KOH has also been widely employed as an activation agent for WS [17,32,37,62,63]. The mechanism of activation of an alkali metal proceeds through implantation of the metal within the carbon lattice where the metal acts an electron donor initiating the reaction during activation [50]. Therefore, creating pores in AC through evaporation of KOH from previously occupied spaces [64]. The intercalation of the metal within the carbon matrix results in a stabilized expansion of spaces between layered carbon atoms enhancing the efficiency of the adsorbent [65]. Ming et al. investigated the effects of carbonization temperature, activation temperature and the impregnation ratio of KOH to WS [17]. It has been reported that increasing the carbonization and activation temperature from 500 to 700 °C increases BET surface area and micropore volume percentage. However, at 800 °C and above, a decline of both BET surface area and micropore volume is observed. The increase in BET surface area and micropore volume is attributed to the continuous evolution of volatile compounds from the precursor that allows for the development of the elementary pore structure of the char. Nonetheless, at extreme temperatures, excessive burn-offs occur reducing the yield of AC. As for the impregnation ratio, BET surface area and micropore volume increase with KOH ratio with an optimum ratio of 3:1 beyond which a decrease is detected. Wu et al. reported that KOH activation promotes pore development and expansion which is demonstrated in the SEM images where it is revealed that KOH activated AC has highly developed overall pores structure and rough surface with a uniform distribution of micropores over the surface [62]. Similarly, Alimohammadi et al. investigated the effect of increasing the KOH impregnation ratio on the chemical activation of WS [57]. It was reported at high KOH impregnation ratios, the shape of the isotherm curve exhibited a typical type IV isotherm indicating a pore size distribution in the mesopore range. The presence of KOH at larger amounts caused stronger release of volatiles in the activation process, thus, converting micropores into mesopores. It has been reported that activation with KOH will result in a positively charged AC which is advantageous for the removal of negatively charged contaminants [66]. Shao et al. successfully

Table 5
Studies that used H_3PO_4 for the activation of WS.

Adsorbate	t (h)	T (°C)	IR (g/g)	S_{BET} (m^2/g)	V_t (m^3/g) x 10^{-6}	q_{max} (mg/g)	Reference
Cu (II)	1	500	2	1433.13	0.9083	34.4	[60]
Malachite green	1.5	450		420.5		11.76	[36]
Phenanthrene	2	700	2	410.84	0.61	247.54	[40]
Reactive red 198	2	550	3.5	1980	1.976	79.15	[57]

synthesized Cu-doped WS-based AC (CU-WS-AC) for the removal of malachite green [67]. In the presented study, WS was mixed with Cu $(CH3COO)_2{\cdot}H_2O$ solution and carbonized at a temperature of 600 °C after which chemical activation with KOH took place. The surface morphology of the adsorbent was characterized using SEM. A large number of dispersed Cu particles are exposed on the surface of the adsorbent indicating the successful introduction of Cu particles. Due to the surface complexation interaction that occurred between Cu^0/Cu^{2+} and the malachite cationic dye, a high adsorption capacity of 2477 mg/g was achieved. Table 6 presents studies that used KOH for the activation of WS.

A comparison study between chemical activation with KOH and H_3PO_4 was performed by Alimohammadi et al. for the removal of reactive red dye 198 [57]. The study was performed with different impregnation ratios ranging from 1 to 3.5. The BET analysis demonstrated that the shape of N_2 adsorption/desorption isotherms is highly affected by the activating agent and the impregnation ration. At lower impregnation ratios, pore structure showed is mostly microporous. However, at higher impregnation ratios, the structure shows a higher percentage of mesoporosity. This phenomenon applied to both activating agents. Conversely, ACs exhibited reverse effects on the specific surface area when altering impregnation ratios. S_{BET} of the KOH revealed an inverse relationship between S_{BET} and impregnation ratio. At high impregnation ratios, lower S_{BET} values were recorded. H_3PO_4 showed a direct relationship between impregnation ratios and S_{BET} values. H_3PO_4 is known to inhibit the formation of tar that acts as barricade towards pore formation. The SEM analysis revealed that both ACs have different structures. KOH AC displayed large holes with a honeycomb surface. According to Boehm titration, samples activated with KOH have more basic groups. FTIR analysis spectra was different for both ACs where the main difference is the characteristic peak of C-H aromatic stretching. Samples activated with H_3PO_4 had carbonyl groups that are relatively intense. KOH activated samples had higher content of aromatic C-H stretches.

Similar to H_3PO_4, $ZnCl_2$ combines with raw biomass material and carbonized biomass and is also widely applied for the production of AC. Chemical activation transpires by the swelling effect of $ZnCl_2$ where inter and intra voids materialize due to lateral bonds breaking in the cellulose molecules, henceforth, microporosity is developed through the interspaces between carbon layers induced by $ZnCl_2$ [50]. In addition, it has been reported that $ZnCl_2$ acts as a Lewis acid [68]. In other words, polymerization reactions occur due to aromatic condensation, initiated by $ZnCl_2$, that allows molecular hydrogen deformation from the hydroaromatic structure of the biomass and thereby creating active sites on adjacent molecules. Although $ZnCl_2$ cultivates a highly porous and well-developed AC, it is not recommended by food and pharmaceutical companies due to it being a hazardous and a non-environmentally friendly material.

Various studies have undergone the $ZnCl_2$ activation with promising results [12,13,69–72]. Teimouri et al. reported the effect of carbonization time and atmosphere on the AC [70]. It was stated that highest carbon yield obtained was at 30 min after which a decline in efficiency was observed. Furthermore, it was reported during carbonization, the rate controlling step of the gas-solid reaction is the diffusion of CO through the porous media. The overall carbonization rate increases when increasing the gasification rate. Nazari et al. also reported the investigation of chemically activated WS using $ZnCl_2$ for the removal of cephalexin where the AC showed a highly porous structure where a remarkable yield of 41.3% was achived [13]. Li et al. reported that due to $ZnCl_2$ activation, the structure of the WS precursor went from being a low-porous structure to being a heterogenous surface filled with ledges and cavities with pores of different sizes and shapes [72]. Table 7 shows the performance and properties of WS-based AC chemically activated with $ZnCl_2$.

It is noteworthy to mention that since $ZnCl_2$ and H_3PO_4 can react with raw WS, the extra step needed to carbonize the precursor which is the case with other chemical activation agents is eliminated, thus, saving energy and time in the process.

Potassium carbonate has also been used for the production of AC from WS [22,73]. In contrast to KOH and NaOH, K_2CO_3 is not harmful if used in food and pharmaceutical supplements. Activation occurs as the potassium compound penetrates into the carbon matrix expanding and creating new pores in the process [74]. Wang et al. performed a study with a two-step activation using K_2CO_3 [73]. Activation was performed by mixing K_2CO_3 with WS and then heated to a temperature of 600 °C with a dwell time of 1 h. The mixture was then heated again to temperature of 800 °C for another 1 h. Resulting SEM images displayed a heterogeneous surface with irregular cavities. Activated WS exhibited a high micropore content. It was stated by Ozcimen et al. that porosity development is highly linked to the raw material of the AC [75]. A higher cellulose content produces more micropores, whereas higher lignin content produces more macropores. WS is a material with high lignin content as such, produced AC from WS is highly macroporous. Wang et al. also noted that AC produced from one-step activation yields a higher total pore volume than that by two-step activation [73]. Teixeira also performed activation of WS using K_2CO_3 for the removal of antibiotics [22]. Table 8 depicts the performance of studies present in the literature review that utilized K_2CO_3 for the chemical activation step. Fig. 5 shows chemical activating agents used for the preparation of AC from WS in the literature - the most commonly used activating agents are Zinc chloride and Phosphoric acid.

The production of quality AC relies heavily on the operating parameters of the activation process. Xu et al. reported that the porosity is heavily influenced by impregnation ratio and activation temperature and less influenced by activation time [76]. Prolonged activation time leads to a disordered arrangement and the formation of intermediates that may block pore or collapse part of pore walls. An increase in the impregnation ratio results in an increase in porosity [77].

Nowicki et al. illustrated the influence of the method of activation, temperature of activation and heating mode on the reactivity of WS-

Table 6
Studies that used KOH for the activation of WS.

Adsorbate	t (h)	T (°C)	IR (g/g)	S_{BET} (m^2/g)	V_t (m^3/g) x 10^{-6}	q_{max} (mg/g)	Reference
Acid red 18 dye	1	800	3	1552	0.78	–	[63]
Hydrogen sulfide	1	700	2	640.9	0.2954	–	[37]
Methanol	1	700	3	1636	0.641	248.02	[17]
Reactive red 198	1	900	1	1439	0.769	79.15	[57]
Malachite green	2	800	1	206.6	0.2602	2477	[46]

Table 7
Studies that used $ZnCl_2$ for the activation of WS.

Adsorbate	t (h)	T (°C)	IR (g/g)	S_{BET} (m^2/g)	V_t (m^3/g) x 10^{-6}	q_{max} (mg/g)	Reference
Corn syrup	0.5	500	1	1000.7	0.4574	–	[70]
Cephalexin	1	450	1	1452.1	0.7151	233.1	[13]
Dimethyl amino ethyl azide liquid fuel	0.5	500	–	1480	0.805	248.02	[71]
Congo red (CR) and methylene (MB) blue dyes	1.5	900	4	1626.96	–	CR: 400.11 MB: 442.56	[72]

Table 8
Studies that used K_2CO_3 for the activation of WS.

Adsorbate	t (h)	T (°C)	IR (g/g)	S_{BET} (m^2/g)	V_t (m^3/g)x10^{-6}	q_{max} (mg/g)	Reference
Sulfamethoxazole	1	Step 1: 600 Step 2: 800	1	725	0.34	135.3	[73]
Sulfamethoxazole (1) + metronidazole (2)	1	900	1	640.9	0.2954	(1): 94 (2): 106	[22]

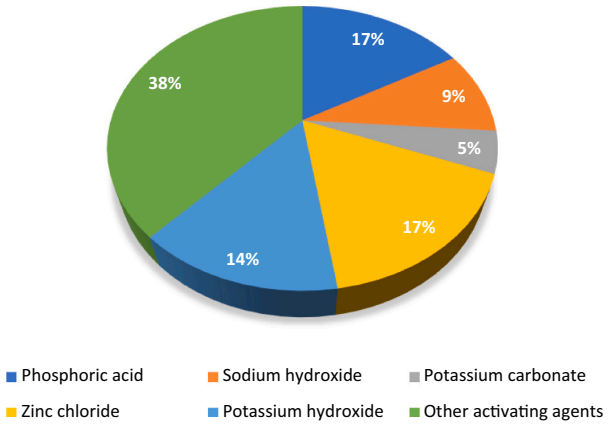

Fig. 5. Chemical activating agents used for the preparation of AC from WS in the literature.

based adsorbents [78]. The resulting activated carbons show that carbon chemically activated with KOH have better textural properties than those physically activated with CO_2. As for temperature of activation, the structural parameters increased with activation temperature regardless of method of activation. In addition, sorption capacities described by the iodine number demonstrated that samples chemically activated have the highest sorption capacities, while physically activated samples were the least effective sorbents. Figs. 6 and 7 represent BET surface area and total pore volume as a function of pyrolysis temperature. It is observed that both entities increase with pyrolysis temperature up to a certain point after which a decreased is observed. This is attributed to the fact that at increasingly high temperatures pyrolysis ceases to occur and the gasification process is initiated instead leading to the disruption of internal pores and a decrease in carbon yield, surface area, and total pore volume. As such, it is not recommended to perform pyrolysis at high temperatures in the case of WS; roughly saying above 600 °C. Table 9 provides a list of research works that used the chemical activation method for the activation process.

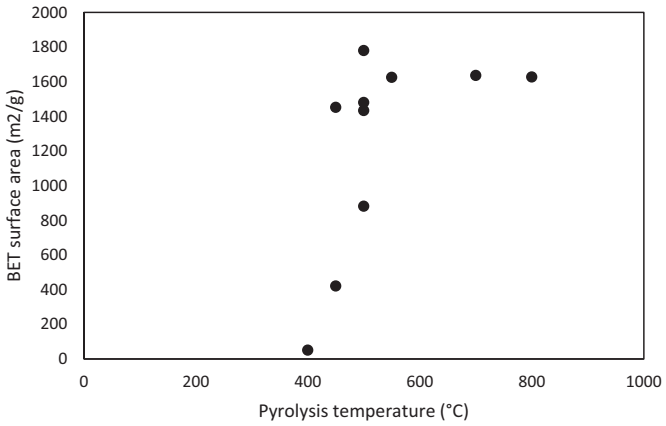

Fig. 6. BET surface area of walnut AC as a function of temperature collected from different studies [10,12,17,34,36,57,60,63,72].

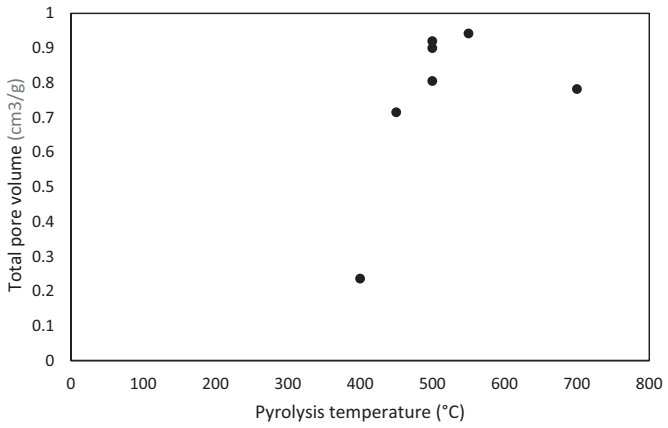

Fig. 7. Total pore volume of walnut AC as a function pyrolysis temperature [12,17,31,34,57,60,71,82].

5.3. Chemical impregnation

Apart from chemical and physical activation, chemical impregnation using different chemical compounds for the improvement of adsorption capacities is also commonly practiced among researchers. Various chemicals have been employed including Maleic anhydride [83], different fatty acids [16], acetic acid [42], epichlorohydrin and alkaline solution [39], titanium and zinc oxide [84], triethylene tetramine [79], triethylamine [85], levulinic acid [81], isopropylidene malonate [35], and diethylenetriamine [86]. Kocaman successfully developed an environmentally friendly approach for the removal of methylene blue dye using WA modified with levulinic acid (LA) [81]. WS were mixed with 0.25 g of LA in n-hexane containing a few drops of sulfuric acid as the catalyst [81]. The mixture was then refluxed at temperature of 65 °C for 8 h. The synthesized adsorbents proved to be efficient in the removal of methylene blue as the adsorption process turned out to be spontaneous with an adsorption capacity of 294.1 mg/g. Faraji et al. effectively introduced quaternary ammonium using epichlorohydrin and trimethylamine to WS [85]. A decrease in the BET surface area and total pore volume was observed due to the presence of amine groups constricting pore channels on the surface of the adsorbent. Liu et al. successfully grafted triethylene tetramine (TETA) onto WS for the removal of Pb^{2+} ions from aqueous solution [79]. Results of the thermal gravimetric analyzer (TG) for both unmodified and modified WS show that the thermal stability enhanced significantly due to strong intermolecular bond energy induced by TETA [79].

Table 10 provides a summary of research works on modified WS using different chemical compounds. It is deduced that chemical modification provides adequate adsorption capacities, however, outstanding morphological properties are produced only through chemical or physical activation [4]. Surface areas, S_{BET}, resulting from chemical activation have reached around 2000 m^2/g, which is similar to commercially available AC produced from WS as specific surface areas of commercially produced ACs typically range from 500 to 2000 m^2/g. This proves that WS-based adsorbents synthesized in the lab can compete against commercially available ones. Another method to enhance the adsorption capacity of agricultural waste is through

Table 9
Adsorption studies underwent chemical activation.

Technique used	Outcome of activation	Contaminant	Effect on adsorption capacity	Reference
Prepared by KOH chemical activation	The S_{BET}, micropore volumeV_m, micropore volume percentage increased to 1636 m^2/g, 0.641 m^2/g and 81.97%	Methanol	The results show that the modified WS is favorable for the adsorption of methanol with adsorption capacity of 248.02 mg/g	[17]
Chemical activation using H_3PO_4 and KOH	H_3PO_4 activation: S_{BET} increased to 1980 m^2/g, PV V_t 1.976 m^3/g and PD 3.99 nm KOH activation: S_{BET} increased to 1625 m^2/g, V_tPV to 0.942 m^3/g PD 2.32 nm	Reactive red 198 dye	Highest adsorption capacity achieved is 1.5 g/g with KOH activation	[57]
TiO2 loaded WS-based activated carbon	S_{BET} increased from 563 m^2/g to 1552 m^2/g Resulting V_tPV: 0.78 cm^3/g And PD: 2.01 nm	Acid red 18 dye	Modified WS exhibited an adsorption capacity of 80 mg/L	[63]
Chemical activation using $ZnCl_2$	S_{BET} increased to 1480 m^2/g and V_t total pore volume of 0.805 cm^3/g	Dimethyl amino ethyl azide	Percentage removal reached up to 85.95%	[71]
Impregnated with $ZnCl_2$ then thermally activated under high-purity nitrogen and flow rate of 300 cm^3/min to a final temperature of 450 °C at a heating rate of 5 °C/min		Cephalexin		[12]
Impregnated with 30% phosphoric acid and then thermally activated under N_2 atmosphere in a furnace at 700 °C for 2 h	Resulting S_{BET}: 410.84 m^2/g V_tPV: 0.61 cm3/g Average PD: 5.92 nm	Phenanthrene	The interactions between the embedded functional groups and phenanthrene played a major role in the 95% recovery	[40]
Chemical activation with ZnCl2	Resulting S_{BET} 1452 m^2/g V_tPV: 0.7151 cm^3/g Average PD: 1.97 nm	Cephalexin antibiotic	Maximum adsorption capacity reached was 233.10 mg/g	[13]
Chemical activation method using concentrated phosphoric acid	The chemical activation resulted in noticeable features such as large S_{BET} 420.5 m^2/g and PD of 2.25 nm	Malachite green	Percentage removal of malachite green reached 100%	[36]
Chemically modified with triethylene tetraamine		Pb(II)	Adsorption capacity increased from 61.16 mg/g to 70.01 mg/g	[79]
Adsorbent prepared by grafting aspartic acid onto WS		Ni(II)	Adsorption capacity of modified WS increased 4 times the unmodified WS adsorbents	[80]
Adsorbent synthesized using solid sodium hyroxide and aspartic acid	S_{BET} increased from 1.04 to 2.33 m^2/g V_t Total pore volume 3.13 to 12.18 cm^3/g Average pore diameterPD increased from 12.09 to 20.92 nm	Reactive brilliant blue	The adsorption capacity increased 18 times	[39]
Fe/Fe3C nanoparticles incorporated onto WS. WS activated through pyrolysis	S_{BET} increased from 1234.9 to 1779.3 m^2/g V_t Total pore volume 0.5to 0.9 cm^3/g	Organic dyes: methylene blue, methyl red, malachite green and methyl orange		[31]
Hydrothermal carbon was produced from WS and chemically activated using nitric acid	S_{BET} increased from 2 to 32 m^2/g V_t Total pore volume increased from 0.004 to 0.114 m^3/g	Methylene blue and malachite green	The adsorption capacity of modified WS increased 4 times that of unmodified	[10]
WS prepared by mixing with oily sludge and then chemically activated using K2CO3	Resulting S_{BET} 725 m^2/g and total V_tPV 0.34 cm^3/g PD 1.87 nm	Sulfamethoxazole	Maximum adsorption capacity reached is 362.9 mg/g	[73]
chemical activation with levulinic acid	S_{BET} increased from 2.81 to 5.29 m^2/g	Methylene blue	Maximum adsorption capacity reached is 294.1 mg/g	[81]
chemical activation by adding KOH via microwave irradiation	S_{BET} 614.24 m^2/g and PD 0.889 nm	Naphthalene and phenanthrene	Maximum adsorption capacity obtained for naphthalene and phenanthrene are 93.62 and 145.62 mg/g respectively	[62]
WS modified with pyrolusite and impregnated with phosphoric acid	S_{BET} increased from 1.15 to 1433.13 m^2/g V_t Total PV increased from 0.0057 to 0.9083 cm^3/g	Cu(II)	Removal of modified WS 20% higher than the un-modified one	[60]
Chemical activation with znCl2	Resulting S_{BET}: 1626.96 m^2/g	Methylene blue and congo red	The adsorbent proved to be effective in removing Methylene blue and congo red	[72]
Walnuts were pyrolyzed in a muffle furnace at a temperature of 400C. then walnuts were loaded with La(OH)3	An increase in S_{BET} from 2.77 to 50.60 m^2/g, V_tPV from 0.002 to 0.236 cm^3/g	Phosphate	Removal efficiency reached a 100%	[34]
Chemical activation with MgCl2	Resulting S_{BET} 25.12 m^2/g, V_tPV: 2.32 m3/g and PD: 52.31 nm	NH_4^+	The uptake capacity of modified WS increased by a factor of 5	[38]
Chemically doped with Cu and then activated with KOH	Resulting S_{BET} 206.6 m^2/g, V_t: 0.2602 m^3/g and PD: 5.038 nm	Malachite green	An uptake capacity of 2477 m^2/g was observed	[46]

introducing conductive polymers. Polyaniline is a prominent example of conductive polymers due to its biocompatibility [87]. Imghran et al. recently created an environmentally-friendly method for industrial wastewater treatment through the synthesis of polyaniline-modified WS biocomposites via in situ chemical polymerization for the removal of orange dye G [87].

6. Effect of operating conditions

The adsorption of contaminants using WS is extensively investigated in the literature under different operating conditions. It was observed from the literature that the parameters that mostly influenced the adsorption process were found to be pH of the solution, temperature, initial concentration of target contaminant, and contact time.

6.1. The effect of pH

Recent peer-reviewed papers indicate that adsorption capacity is highly influenced by pH of the solution. Adsorption can be affected significantly by the surface properties of the adsorbent. Consequently, using raw WS or chemically modifying them will have a huge impact on the adsorption capacity when altering pH of the solution. Depending on the point zero charge potential (PZC). The surface of the adsorbent can be positively charged or protonation of functional groups on the active sites of the adsorbent occurs when pH of the solution is lower than the PZC or negatively charged or deprotonation of functional groups on the active sites of the adsorbent occurs when the pH of the solution is higher than PZC. Depending on the charge of the target contaminant, either electrostatic repulsion occurs leading to a depletion in the adsorption uptake or electrostatic attraction is induced between the adsorbent and adsorbate leading to an increase in the adsorption uptake [89]. Almost one quarter of the WS studies have employed WS without prior activation or modification [43,44,90–104]. For the removal of organic compounds similar results were reported where the adsorption process is strongly pH dependent. Miyah et al. investigated the removal of three dyes of different net charges; methylene blue, crystal violet cationic dyes, and methyl orange an anionic dye [102]. The results demonstrated at acidic pH values, pH range from 2.5 to 5.5, adsorption efficiency was low towards cationic dyes and high towards the anionic dye. Studies that investigated the removal of methylene blue reported maximum adsorption at high pH values, ranging from 6.5 to 12 [90,92,98]. Being a cationic dye, electrostatic repulsion between methylene blue and positively charged adsorbent occurs at low pH values subsequently reducing the adsorption capacity.

The effect of altering the pH of solution on the removal of heavy metal ions has also been extensively investigated in the literature. Effect of influence of pH on Cr(IV) adsorption was investigated by Banerjee et al. [44]. The results showed a maximum adsorption capacity at pH 2 the reason being at low pH values $HCrO_4^-$, $Cr_3O_{10}^{2-}$, $Cr_2O_7^{2-}$ are present in the solution thus, creating a positive impact on the adsorption capacity due to attractive forces between the negatively charged ions and the positively charged surface of the WS adsorbent. Similarly, Celebi et al. evaluated the removal of lead ions using WS and maximum adsorption capacity was achieved at low pH values from 2 to 6 [94]. Optimum pH value determined was 4 after which a decreased in adsorption capacity was observed. An opposing finding has been reported by Najam et al. for the removal of Cu(II), Zn(II) and Cd(II) [97]. All three divalent cationic metals prevailed an increase in adsorption capacity while increasing the pH of solution. The adsorption of heavy metal ions is the result of the presence of functional groups such as ketones, aldehydes, amines, phenols, alcohols, and carboxyl groups that are normally found on the surface of the WS. These groups tend to protonate at lower pH values and hence, uptake of metals is low. Faraji et al. studied the influence of pH on the removal of phosphate ions [85]. The results revealed that an increase in adsorption capacity from pH 4 to 6 after which a decrease in capacity was reported beyond pH 6. This is attributed to the fact that deprotonation occurs at high pH values resulting in a decline in the electrostatic interactions in turn reduction in the uptake of phosphorous ions.

Overall, it is concluded that the adsorption capacity is strongly influenced by pH of solution due to its influence on the surface charge of the adsorbent and the degree of ionization and speciation of the adsorbate.

6.2. The effect of temperature

Many researchers have reported the increase in the adsorption capacity with temperature emphasizing the endothermic nature of the adsorption process using WS-based adsorbents. Miyah et al. reported that the adsorption capacity increased with increasing temperature [92]. It was mentioned that the adsorption process is endothermic in nature and the increase in adsorption capacity is due to the increase in mobility of the adsorbate at higher temperatures. For the removal of cationic heavy metal ions, adsorption capacity increases with increasing temperature. Najam et al. also investigated the influence of temperature on the removal of Cu(II), Zn(II) and Cd(II). It was reported that adsorption process is endothermic in nature and the resulting Gibb's free energy is negative indicating that WS has high affinity towards heavy metal ions. Pazouki et al. studied the effect of temperature ranging from 25 to 45 °C for the removal of mercury and the results indicated that the removal efficiency increased with increasing temperature displaying an endothermic nature of the adsorption phenomenon [51]. Li et al. also investigated the effect of temperature on two types of dyes – congo red and methylene blue and the results implied that the removal of dyes is strongly affected by the temperature of the solution [72]. Both dyes exhibited the same outcome stating that the dye adsorption capacity increased with temperature. The interpretation of the given result was that the diffusion of dyes within the adsorbent increases giving way to more incessant interactions between dye molecules and active sites on the surface of the adsorbent.

Thermodynamic parameters are evaluated to study the effect of temperature on the adsorption behavior on WS-based adsorbents. These parameters include Gibbs free energy, ΔG, enthalpy, ΔH, and entropy, ΔS. Many research works have assessed and reported the values of those parameters in the literature. Nazari et al. reported negative ΔG values between −4.96 and − 9.51 KJ/mol ΔH for the removal of cephalexin antibiotic [12]. Negative values indicate that a spontaneous physisorption took place and the increase in negative values with temperature is an indication of the degree of spontaneity with temperature. The endothermic nature of the process was confirmed with the determined positive value of ΔH. The outcome of this research has been supported by the work of other researchers where a negative ΔG value and a positive ΔH value were evaluated indicating a spontaneous and endothermic adsorption process [58]. On the contrary, Zheng et al. and Lie et al. reported negative ΔH values implying that the adsorption process is exothermic in nature and that adsorption decreases with temperature [32,40]. In addition, Ozdemir et al. investigated the effect of temperature on the adsorption of methylene blue on WS [104]. It was reported that the adsorption efficiency decreased with increasing temperature [104]. A similar finding was reported by Tang et al. stating that the adsorption is exothermic in nature [90].

6.3. The effect of ionic strength

It is well documented that ionic strength influences the adsorption process onto WS. Ionic salts are known to participate in mechanisms and interactions that involve target molecules in solution and adsorbent surface in addition to altering the charge of the adsorbent surface [105]. From the literature, two distinct phenomena are recorded that can describe the effect of ionic strength on the adsorption process onto WS-based adsorbents. The first effect depends on the electrostatic nature and configuration of the target contaminant. Second, the increase in salt

Table 10
Adsorption studies on chemically modified WS.

Technique used	Outcome of activation	Contaminant	Effect on adsorption capacity	Reference
Chemical activation method using acetic acid alone and a mixture of acetic acid and hydrogen peroxide	S_{BET} decreased from 1.2 to 0.9 m^2/g and pore diameterPD increased from 11.84 to 19.85 nm	Methylene blue, Methyl violet, Murexide, and Fe3+ and Cu2+	Raw WS had the highest adsorption capacity towards Fe^{3+} and Cu^{2+} However, adsorption capacity improved towards Methylene blue, Methyl violet, and Murexide	[42]
Fatty acid modified (capric acid (CA), lauric acid (LA), palmitic acid (PA) and oleic acid (OA)) through esterification in n-hexane with sulfuric acid as catalyst	S_{BET} increased from 2.79 m^2/g using: CA: 4.28 m^2/g LA: 4.15 m^2/g PA: 4.05 m^2/g OA: 4.32 m^2/g	Naphthalene	With the fatty acid treatment, the adsorption capacities of modified WS improved significantly	[16]
Chemical modification with Zinc Oxide and Titanium Oxide	–	Humic acid	Adsorption capacity of raw WS increased from 35.2 mg/g to WS modified with Zinc oxide 37.9 mg/g and WS modified with Titanium oxide to 40.2 mg/g	[84]
Impregnation of magnetic particles on calcinated particles of WS-rice husk	S_{BET} increased from 38.08 to 126.72 m2/g, V_tPV increased from 0.0073 to 0.0811 cm3/g average pore diameterPD increased from 0.277 to 0.418 nm	Cd(II)	The modified adsorbent was effective in the removal of Cd(II) with percentage removal of 80%	[45]
Chemical modification by grafting with sulfur containing functional groups using xanthate	S_{BET} increased from 49.9 to 208 m^2/g V_tPV increased from 0.076 to 0.164 cm^2/g	Pb(II)	The percentage removal at optimum conditions increased from 53.3 to 99.7%	[88]
Modification with levulinic acid	S_{BET} increased from 2.81 to 5.29 m^2/g	Methylene blue dye	Resulting adsorption capacity 294.1 mg/g	[81]
Chemically modified using epichlorohydrin and trimethylamine to produce quaternary ammonium groups	S_{BET} decreased from 4.96 to 2.27 m^2/g V_tPV decreased from 0.0076 to 0.0034 cm^3/g	Phosphorus	Maximum adsorption capacity reached 22.73 mg/g	[85]

concentration can induce an effect that is termed as “squeeze out” effect where excess salts penetrate into the inner pores of the carbonaceous adsorbent repelling the interactions between the adsorbate and adsorbent [106]. Moreover, positive ionic salts can neutralize the negative charge of both adsorbents and adsorbates weakening the electrostatic interactions between them thus, decreasing the adsorption capacity [106].

Several studies reported that the presence of cations affected the adsorption capacity negatively. Miyah et al. and Tang et al. recorded a decrease in adsorption efficiency for the removal of methylene blue in the presence of cations [90,102]. Methylene blue is a cationic dye and it is only natural for cationic ions such as Na^+ to compete against the cationic dye for active sites on the adsorbent resulting in a deficiency in methylene blue uptake. A similar finding has also been reported by Li et al. for the removal of hexavalent chromium [86]. The presence of salts in the solution resulted in a negative impact on the uptake of chromium where it is perceived that ions in the solution compete against Cr(VI) for the adsorption sites on the surface of the adsorbent weakening the electrostatic attraction between the adsorbent and the chromium ions. Luo et al. studied the effect of coexisting ions for the adsorption of phosphate using WS-based adsorbent modified with lanthanum chloride and sodium hydroxide [34]. Anions tested include Cl^-, NO_3^-, CO_3^{2-} and SO_4^{2-} all of which had no significant impact on the adsorption capacity except for SO_4^{2-} ion which interfered with adsorption of phosphate.

7. Adsorption mechanisms

The mechanism of adsorption onto activated WS can be generally classified into physical and chemical adsorption where each category is based on the nature of interactions and affinity of target contaminant towards various functional groups. For instance, chemical adsorption is mediated by chemical reaction or the bonding of adsorbate and functional groups imbedded on the surface of the adsorbent. These types of interactions are profound, and the adsorbent can undergo chemical changes, which are irreversible and not favored for regeneration due to high energy requirement. On the other hand, physical adsorption is governed by the weak Van der Waals interactions between target contaminant and the adsorbent, and the adsorbent does not undergo chemical changes. Other mechanisms for the adsorption onto WS-based adsorbent include hydrogen bonding, ion exchange and electrostatic interactions.

Adsorption mechanisms are highly influenced by the characteristics of the adsorbate and the chemistry of the background solution. Uddin et al. reported a low adsorption capacity at low pH values and high adsorption capacity at high pH values for the removal of methylene blue dye using raw WS [98]. The major interaction responsible for the removal is electrostatic interactions between the cationic dye and the functional groups on the surface of the adsorbent. pH values higher than PZC results in a negatively charged surface, thus intensifying the attraction forces towards Methylene blue. Methylene blue is a cationic dye and as such, it is only natural an electrostatic attraction is induced between a positively charged entity and a negatively charged surface. The influence of pH on the adsorption of alizarin yellow GG on carbonized WS-based adsorbent has been investigated by Kaya et al. [107]. In contrast to methylene blue dye, alizarin yellow GG is an anionic dye hence, maximum adsorption capacity was achieved at pH value of 3 due to the heightened electrostatic interactions between the anionic dye and the positively charged surface of the adsorbent. To determine whether other interactions are involved in the adsorption process, studies were carried out at PZC to eliminate the involvement of electrostatic interactions due to surface charge. However, turns out that electrostatic interactions are solely or majorly responsible of the adsorption of the anionic dye. This is attributed to the fact that negatively charged particles are naturally attracted to negatively charged surfaces and positively charged particles are normally attracted to negatively charged surfaces [107].

It is possible that the adsorption process is a result of synergetic effect of several interactions occurring simultaneously. Zhou et al. stated that

Π-Π electron-donor-acceptor (EDA) mechanism for the adsorption of methylene blue onto WS magnetized with double salt of ammonium ferrous sulfate (DS-AC) [31]. DS-AC acted as an electron donor due to its high Π-electron density and methylene blue is a Π-electron acceptor, henceforth, inducing the Π-Π electron donor acceptor interactions resulting in the adsorption of methylene blue. Moreover, strong Van der Waals contributed to the adsorption process due to the interaction between sp^2-hybridized carbon with high Π-electron density domain of DS-AC and the Π-electron acceptor of the aromatic ring structure of methylene blue. In addition to these mentioned interactions, Zhou et al. proposed the presence of Fe/Fe3C particles in addition to the hierarchically porous structure which collectively enhanced the electron transfer through Fe/Fe_3C particles to Fe^{2+}, while the generated H+ from 2H+/H2O could accelerate the dissociation of methylene blue. The mechanism is explained through chemical reactions 1 through 4 starting with the adsorption of methylene blue onto the surface of the material followed by the release of Cl^- ions through the reaction of methylene with Fe/Fe_3/C species. Then, the release of Fe2+ and active H^+ due to the combination of ionic H+ and Fe/Fe3C/C particles. Finally, decolorization reaction occurs.

$$Fe/Fe_3C/C + MB^{\sigma} + Cl^{\sigma-} \Rightarrow Fe/Fe_3C/C/MB^{\sigma+}Cl^- \quad (1)$$

$$Fe/Fe_3C/C + MB^{\sigma+}\ Cl^{\sigma-} + e^- \Rightarrow Fe/Fe_3C/C/MB + Cl^- \quad (2)$$

$$Fe/Fe_3C/C + 2H + /H_2O \Rightarrow Fe^{2+} + 2H^* + 2OH^- \quad (3)$$

$$Fe/Fe3C/C/MB + H^* \Rightarrow Fe/Fe3Fe/C + \text{redox reaction products} \quad (4)$$

Qiongfen et al. was able to deduce from the adsorption isotherms and thermodynamic that the phosphine adsorption onto metal oxide-modified WS-AC (MWAC) is chemical in nature [108]. According to the thermodynamical equilibrium analysis, PH_3 will react with O_2 to produce H_3PO_4 and small amounts of $(P_2O_5)_2$ when the molar ratio of O_2 to PH_3 in the solution is 2 and above. The presence of CuO loaded onto the MWAC plays a major role in acting as an oxygen carrier in the PH_3 adsorption-oxidation process. Possible mechanisms proposed for the study are presented in chemical reactions 5 through 10. The adsorption-oxidation process is initiated by the physical adsorption of PH_3 and O_2 onto the active site of the adsorbent as presented reactions 5 and 6. Eqs. (7) and (8) present the rapid reaction that occurs between the lattice oxygen of the active components on the surface and adsorbed PH_3 species to form H_3PO_4 and P_2O_5. The produced P_2O_5 species consequently react with water to form H_3PO_4 as seen in reaction 9. Finally, reaction 10 depicts the adsorption of generated P_2O_5 and H_3PO_4 onto the adsorbent. It is noteworthy that the high adsorption capacity of PH_3 is due to the combined effects of the large surface area, 1419 m^2/g, in addition to the high oxidation activity of MWAC adsorbent in PH_3 adsorption-oxidation to H_3PO_4 and P_2O_5.

$$PH_3 + X \Leftrightarrow PH_3\text{–}X \quad (5)$$

$$O_2 + X \Leftrightarrow O_2\text{–}X \quad (6)$$

$$PH_3\text{–}X + 4\ OM \Leftrightarrow H_3PO_4\text{–}X + 4\ M \quad (7)$$

$$4PH_3\text{–}X + 16OM \Leftrightarrow (P_2O_5)_2\text{–}X + 6H_2O + 16\ M \quad (8)$$

$$(P_2O_5)_2\text{–}X + 6H_2O \Leftrightarrow \$H_3PO_4\text{–}X \quad (9)$$

$$2\ M + O_2\text{–}X \Leftrightarrow 2OM + X \quad (10)$$

Π-Π interactions resulting from the alteration of the adsorbent's surface chemistry is a primary enhancement element in the adsorption process. Zheng et al. investigated the adsorption mechanism of phenanthrene dissolved in surfactant polysorbate 80/tween 80 using WS chemically activated with H_3PO_4 [40]. The results of the XPS analysis confirmed the presence of oxygen containing functional groups which was further confirmed by the results obtained from Boehm titration. The Π-Π bonding occurs between C═C double bonds or benzene rings of both the adsorbent and phenanthrene molecules. The occurrence of the Π-Π interactions was verified through the FTIR analysis of the spent adsorbent where a shift and enhancement of the intensity of C═C stretching of aromatic rings was observed. Additionally, Π-Π* transitions in the aromatic rings signify the existence of Π electron on the surface of the adsorbent due to the adsorption of phenanthrene which further cements the crucial role of Π-Π interactions in the adsorption process.

Wang et al. suggested a holistic approach for the adsorption of sulfamethoxazole onto activate WS that includes three types of mechanisms including dispersive interaction of Π-Π electron coupling between the graphitic structure of the AC and the aromatic rings of sulfamethoxazole, the electron donor-acceptor interaction between phenol aromatic ring of the contaminant and the oxygen functional groups on the surface of the AC, and the large S_{BET} and pore size distribution [73]. Fig. 8 provides a brief illustration of the adsorption mechanism of sulfamethoxazole onto modified WS.

In addition to electrostatic interactions, pH also plays a key role in hydrogen bonding, electron exchange, and Π-Π dispersion interactions in solution [109]. Luo et al. proposed that the mechanism of phosphate onto $La(OH)_3$ nanorod/WS biochar composite (LN-WB) is a combination of electrostatic interactions, surface precipitation and ligand exchange [34]. Maximum adsorption capacity occurred at high pH values where all three forms of mechanisms took place. Phosphate ions exchanged positions with OH- and CO_3^{2-} ions through ligand exchange. At low pH values, adsorption capacity decreased as electrostatic interactions ceased to occur in addition to the deprotonation of La-OH and the replacement of OH- and CO_3^{2-} ions. Fig. 9 provides a brief schematic diagram of the proposed adsorption process.

To conclude, electrostatic interactions, Π-Π and Π-Π EDA interactions, surface precipitation, ligand exchange/ions exchange are all important mechanisms for the adsorption onto WS-based adsorbents. Therefore, providing a good analysis of the mechanism acquires a thorough characterization of both the adsorbent and adsorbate. In addition, nature of the background solution needs to be taken into consideration given that pH is a major key role player in the adsorption process. Furthermore, surface functional groups also take part in the mechanism adsorption and the uptake efficiency.

8. Modeling of adsorption on WS

8.1. Adsorption isotherm modeling

Adsorption is a phenomenon that can be briefly described by the transfer of substances from mobile phase, liquid or gaseous, to a solid phase [110,111]. Thus, in order to describe and predict the mobility of these substances, adsorption isotherm curves are utilized. Essentially, isotherm curves govern the retention of liquid/gas adsorbates on solid adsorbents while varying initial concentrations of target contaminant at predetermined operating conditions [111,112]. Furthermore, isotherm curves provide insights into the adsorbent's surface properties, adsorption mechanism and the degree of affinity during the adsorption process. There are several empirical models used, however, the focus will be on two commonly used isotherm models, the Langmuir and Freundlich isotherms as they were adopted in various sorption studies in the literature to determine the maximum adsorption capacities and predict the type of adsorption mechanism.

The Langmuir model is given by Eq. (11) [113].

$$q_e = \frac{q_{max} b C_e}{1 + bC_e} \quad (11)$$

where q_e is the amount adsorbed at equilibrium per unit weight of adsorbent (mg/g), C_e is the equilibrium concentration of adsorbate in

the liquid phase (mg/L), q_{max} and b are the Langmuir constants and are referred to as the maximum adsorption capacity (mg/g) and affinity parameter of the adsorption system.

Equations are often linearized for ease of plotting and is given by Eq. (12):

$$\frac{1}{q_e} = \frac{1}{bq_{max}C_e} + \frac{1}{q_{max}} \quad (12)$$

The assumptions of employing the Langmuir isotherm include a homogenous adsorption process, in other words, the model assumes the adsorbent has a uniform surface with equivalent adsorption sites. As in, each molecule has the same activation energy, no lateral interactions between neighboring adsorbed molecules, and no immigration of molecules on the surface of the adsorbent [115].

The Freundlich isotherm is expressed using Eq. (13) where K_f is the Freundlich parameter that expresses the amount adsorbed (mg/g)(L/mg)$^{1/n}$ and n represents the adsorption strength [114]. The value of 1/n ranges between 0 and 1. Values below 1 imply chemisorption and values above 1 indicate a cooperative adsorption. Unlike Langmuir isotherm, Freundlich models assumes a multilayer adsorption with uneven distribution of heat and affinities over a heterogeneous surface energies [89]. This isotherm model is criticized for its inability to abide by Henry's law at low concentrations of the target contaminant [116]. The Freundlich model is given by Eq. (13):

$$q_e = K_f C_e^{1/n} \quad (13)$$

The corresponding linear form is given by Eq. (14):

$$lnq_e = lnK_f + \frac{1}{n} lnC_e \quad (14)$$

Table 11 provides both empirical isotherm models applied to adsorption data in studies available in the literature for the adsorption of different contaminants on the WS-based adsorbents. Adsorption isotherms are useful tools for the prediction of the relationship between the uptake capacity of the adsorbent and its equilibrium concentration in the aqueous phase. Uddin et al. applied three isotherm models including Langmuir, Freundlich and Dubinin-Radushkevitch to investigate the adsorption process of methylene blue onto powdered WS [98]. Studied models were plotted in order to investigate the linear plots. Parameters belonging to the isotherm models were determined from the slope and intercept. It was deduced from the mathematical calculation of the experimental results that the Langmuir isotherm was the best fitted model. Moreover, it can be concluded from the Langmuir model that the adsorption mechanism of methylene blue onto powered WS is chemisorption in nature. Hsini et al. applied Langmuir and Freundlich isotherms to evaluate the maximum adsorption capacity and to have an insight into the distribution of Cr (VI) onto the active sites of the adsorbent using two synthesized adsorbents arginine-doped polyaniline (Arg-PANI@WNS) WS and WS modified with polyaniline in the absence of arginine (PANI@WNS) [117]. The latter isotherm resulted in a better fit than the former with a higher correlation value of 0.9901 and 0.9913 for Arg-PANI@WNS and PANI@WNS respectively. This finding suggests the Cr (VI) adsorption follows a multilayer pattern on a heterogenous adsorbent surface for both adsorbents. A new adsorption isotherm regional analysis model (ARIAN model) introduced by Samiey was employed in this study [118,119]. ARIAN model follows the assumption that the adsorption process constitutes of four distinct regions. The first region satisfies Henry's law at low concentration ranges where the adsorption capacity against adsorbate equilibrium concentration is linear plot. The second phase represents the conventional Langmuir isotherm or Tempkin where adsorption occurs in the form of a monolayer on the surface of the adsorbent. The third region corresponds to the formation of the second layer of adsorbates on the surface of the adsorbent where the analysis of the equilibrium data is performed using the bilayer isotherm. The fourth and last region depicts the adsorption system reaching a saturation plateau including reverse desorption. The adsorption data of the study did not comply with Henry's law as the equilibrium data exhibited a non-linear trend. The equilibrium data showed a good compatibility with the second and third regions starting with concentrations 140.34 mg/L and 118.12 mg/L for PANI@WNS and Arg-PANI@WNS respectively. Finally, the fourth region was not perceived as the equilibrium plateau was not reached. This result translates that the adsorption of Cr (VI) onto PANI@WNS and Arg-PANI@WNS portrays a multi-region profile that demonstrates there are different binding sites due to amine and imine groups originating from PANI and arginine on the surface of the adsorbent.

Liu et al. investigated four isotherm models, Langmuir, Freundlich, Temkin and Dubinin-Radushkevich to evaluate the adsorption behavior of naphthalene on commercial activated WS [32]. The results suggested the following order of best fitting according to R^2 values: Fruendlich > Langmuir > Temkin > Dubinin-Radushkevich. Moreover, Freundlich parameters were calculated, and it was determined that the adsorption of Naphthalene onto activated WS was a favorable one considering 1/n value lies within the range 0.1 and 3. The findings also reveal that the

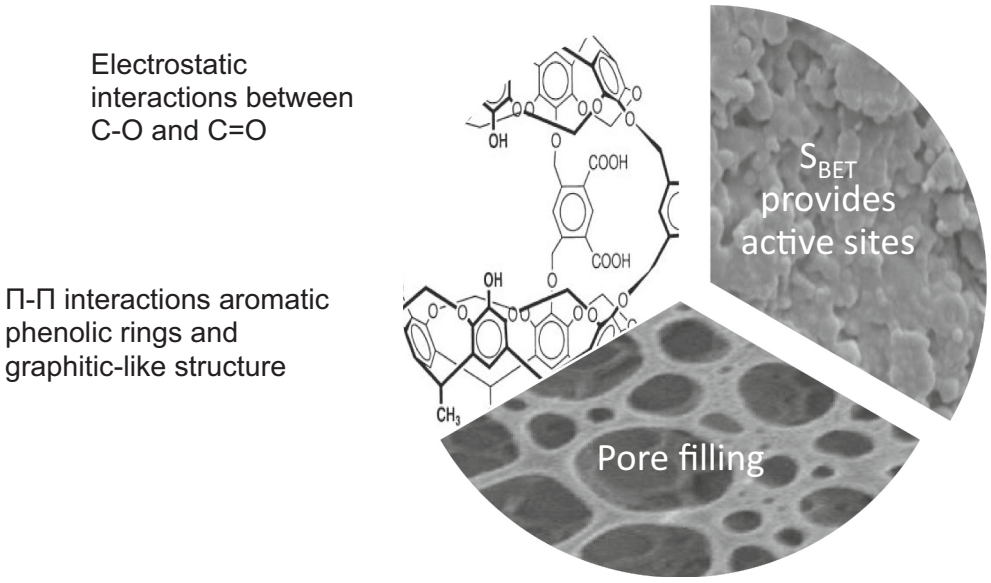

Fig. 8. Adsorption mechanism of sulfamethoxazole onto modified walnut shell.

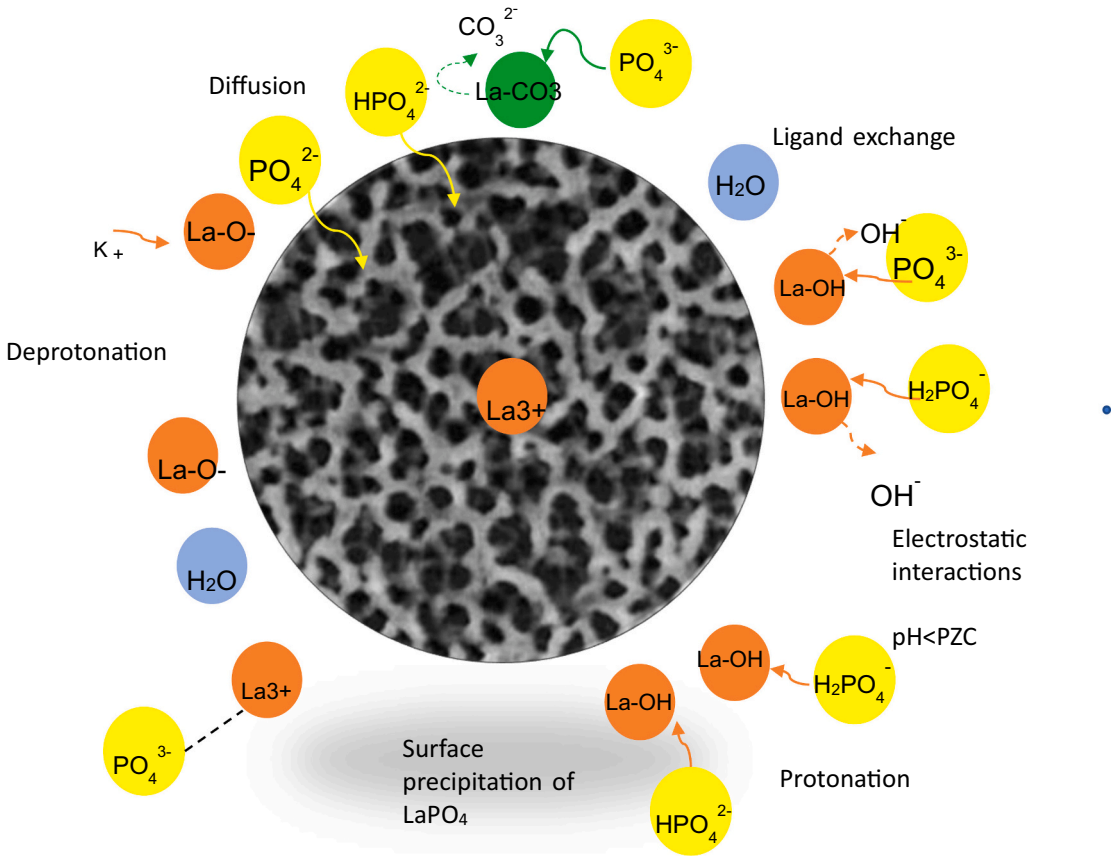

Fig. 9. Schematic diagram of the mechanism of phosphate onto LN-WB.

Freundlich constant, K_f, decreased with temperature signifying that the adsorption of Naphthalene is an exothermic process. Conversely, Kaya et al. examined two isotherm models, Langmuir and Freundlich models by varying the temperature for the adsorption of alizarin yellow GG dye on raw WS [107]. Linear plots of C_e/q_e vs. C_e and ln q_e vs. ln C_e were retrieved at three different temperatures, 25, 35 and 45 °C. The results displayed that the Freundlich model has a better fit according to the R^2 value. The Freundlich constant increased with temperature implying that the adsorption process is endothermic in nature and 1/n value indicated that the adsorption of alizarin yellow is favorable in all experimented temperatures.

8.2. *Adsorption kinetic modeling*

Adsorption equilibrium and kinetics are employed in the design and scale-up of the adsorption systems. The development of kinetics is highly dependent on the theoretical complexity of the adsorption mechanisms [120,121]. Experimental kinetic data is collected by varying contact time for the adsorption process. Various models have been developed to predict the uptake rate of the adsorption system where the Pseudo-first order and Pseudo-second order are the most commonly used models in liquid phase adsorption studies. Pseudo-first order is proposed by Lagergren for the adsorption of oxalic and malonic acid onto charcoal and is expressed as in Eq. (15) [122].

Table 11
Adsorption isotherms and their parameters for the adsorption of different contaminants on WS-based adsorbents.

Adsorbent	Contaminant	Langmuir isotherm			Freundlich isotherm			References
		q_m (mg/g)	K_L (L/mg)	R^2	K_F $mg^{(1-1/n)}L^{1/n}/g$	n	R^2	
Raw WS	Methylene blue dye	36.63	0.054	0.961	2.762	1.56	0.94	[98]
Raw WS	Alizarin yellow GG	4.92	0.195	0.968	15.91	2.38	0.95	[107]
Carbonized WS	sulfamethoxazole	135.3	0.025	0.999	15.4	2.73	0.89	[73]
WS impregnated with Fe/Fe_3C nanoparticles	Methylene blue dye	641	0.001	0.999	6.286	9.93	0.89	[31]
WS chemically activated by K_2CO_3	Metronidazole	107.4	2.6	0.979	60.8	4.5	0.92	[22]
WS chemically activated by K_2CO_3	sulfamethoxazole	93.5	22.2	0.972	65	5.5	0.83	[22]
Chemically modified by NaOH	Phosphorous	22.73	0.04	0.94	1.57	1.88	0.98	[85]
Chemically modified Levulinic acid WS	Methylene blue dye	294.1	0.012	0.949	0.073	1.61	0.98	[81]
Carboxylate-functionalized WS	Pb^{2+}	192.3	0.36	0.994	106.64	8.16	0.94	[35]
Arginine-doped polyaniline WS	Cr (VI)	562.8	0.03	0.917	110.85	3.55	0.99	[117]
Diethylenetriamine modified WS	Cr (VI)	50.1	0.034	0.998	–	–	–	[86]
WS modified with titanium dioxide	Humic acid	34.42	0.04	0.95	2.22	1.49	0.94	[84]
WS modified with zinc oxide	Humic acid	18.59	0.11	0.65	2.66	1.80	0.79	[84]
WS modified with aspartic acid	Reactive brilliant blue dye	201.5	0.008	0.99	8.67	2.08	0.95	[39]
Commercial activated WS	Naphthalene	243.9	0.211	0.96	43.66	1.77	0.99	[32]
WS chemically activated with $ZnClL_2$	Dimethyl amino ethyl azide	166.7	0.102	0.89	18.433	1.87	0.96	[71]

$$q_t = q_e - q_e e^{K1t} \quad (15)$$

Linearizing Eq. (15) yields Eq. (16):

$$ln(q_e - q_t) = lnq_e - K_1 t \quad (16)$$

q_e (mg/g) and q_t (mg/g) parameters represent adsorption capacities at equilibrium and time t respectively, and K_1 represents the rate parameter (1/min). Pseudo-first order is known to be valid after the system has been running for long periods of time - when the adsorption system is nearing equilibrium and at the initial stage of the adsorption [123]. This model is applied to interpret data at small time intervals.

Pseudo-second order is used for large intervals, and it predicts that the adsorption rate is second order function with respect to available active sites [124]. It is represented mathematically in the form of Eq. (17):

$$q_t = \frac{K_2 q_e^2 t}{1 + K_2 q_e t} \quad (17)$$

Eq. (18) represented the linearized of Pseudo-second order model:

$$\frac{t}{q_t} = \frac{1}{K_2 q_e^2} + \frac{t}{q_e} \quad (18)$$

where K_2 is the rate parameter in g/mg/min. These model parameters are empirical constants with no distinct significance as no research works have been implemented to identify their underlying physicochemical phenomena when model fitting is finalized [120]. The purpose behind fitting these models into kinetic studies is merely to compliment the adsorbent evaluation.

There are other kinetic models used in the literature including the Elovich equation and the Weber-Morris intraparticle diffusion model. The compatibility of each model relies on several key factors including the characteristics of the adsorbent and adsorbate and the operating conditions. Many research works demonstrated multilinear curves within a studied time frame which depicts that multiple mechanisms can occur simultaneously with a controlling mechanism such as intraparticle diffusion or the transport of the adsorbate to the external surface of the adsorbent. Li et al. performed a kinetic and equilibrium study for the removal of reactive brilliant blue using WS modified with epichlorohydrin and alkaline solution of aspartic acid [39]. The findings revealed that the adsorption obeyed the Pseudo-seconder model where the calculated q_e deviated the least from the experimental one. It is also shown that as the temperature increased, the deviation gap decreased between q_e calculated and the experimental value reaching complete compatibility between the two values. Moreover, the initial adsorption rate increased with temperature and the time required to reach 50% of the adsorption capacity decreased with temperature proving that faster adsorption rates take place at higher temperatures. Naghiadeh et al. modified WS using titanium oxide and zinc oxide for the removal of humic acid from aqueous solutions [84]. Pseudo-first and Pseudo-second models were applied to experimental data at different initial concentrations and the adsorption process was best described by latter model. In addition, the correlation R^2 for the Pseudo-second model was excessively higher for both adsorbents. It was demonstrated that the adsorption capacity increased with an increase in the initial concentration of humic acid. Liu et al. also applied Pseudo-first and second models to experimental data using amino-modified WS for the removal of Pb^{2+} ions [79]. Similarly, Pseudo-second order model also gave the best fit with R^2 equal to 0.999. Data where fitted to the linear forms of the equations where the plot of the Pseudo-second model portrayed a perfect straight line suggesting an agreement between the experimental and model values. It was also indicated that chemisorption is the rate-limiting step of the adsorption process.

Halysh et al. studied the removal of methylene blue using WS modified with acetic acid and a mixture of acetic acid and hydrogen peroxide [42]. Experimental data were applied to validate different kinetic equations including Pseudo-first and second order and the intraparticle diffusion model. The most compatible model according to the magnitude of R^2 and slight deviation of q_e experimental from theoretical is Pseudo-second order model. The resulting R^2 value, 0.873, of the intraparticle diffusion model indicates the adsorption of methylene blue onto modified WS is a multi-step process consisting of the dye adsorption on the surface and pore interior diffusion. Luo et al. developed a $La(OH)_3$ nanorod/WS biochar for reclaiming phosphate [34]. Three kinetic models were applied, Pseudo-first, Pseudo-second and intraparticle diffusion models. The kinetic parameters suggested that Pseudo-second order yields a better fit to describe the kinetics for phosphate removal. Moreover, data were applied to the linear form of the intraparticle diffusion model where the fitting lines did not pass through the origin implying that the internal diffusion is not the rate-limiting step. The fitting curves were divided into two parts emphasizing that the adsorption of phosphate is a multistage process. The parameters of the model indicated the rate of the first stage was greater the second step. Hsini et al. evaluated the mass transfer mechanism of the adsorption process by applying experimental data to the intraparticle diffusion model for the removal of Cr(VI) using arginine-doped polyaniline WS [117]. According to the model, the adsorption process took place in three consecutive steps. The first step involves the mobility of Cr (VI) ions from the solution to the external surface of the adsorbent. The second step, slower than the former one and controlled by rate of diffusion, constitutes of the penetration of Cr (VI) into the internal surface of the adsorbent. Finally, the third step consists of the final adsorption equilibrium phase. Li et al. only applied the Pseudo-second order to study the kinetics of Cr (VI) uptake using unmodified and modified WS with diethylenetriamine [86]. Non-linear regressive analysis was applied to fit the experimental data and modified WS showed a better fit that the unmodified one. Considering that modified WS has higher S_{BET} area and pore volume, the results indicate that morphological properties of the adsorbent are also responsible for fast adsorption rates. The results depicted that the initial reaction stage increased rapidly while the second stage showed a decrease in the reaction rate. This is attributed to the fact that at initial stages of the reaction, Cr (VI) species occupy empty sites promptly. During the second stage, less active sites become available decelerating the reaction rate until equilibrium is reached.

It is safe to say that there is no distinct correlation between the validity of kinetic models and target contaminants, whether organic compounds or heavy metal ions. Furthermore, Pseudo-second order is preferred over other kinetic models given that it is the most applied model in adsorption studies found in the literature to determine adsorption rates and capacities of studied adsorbents. Kinetic models and their parameters for the adsorption of different contaminants on WS-based adsorbents are presented in Table 12.

9. Industrial applications of WS

In addition to bench-scale laboratory works, WS have also been utilized in the industry. Schlumburger designed a produced water downflow filtration system employing WS media filtration [125]. As the liquid passes through the WS bed, oils and suspended solids are proficiently retained by the filter. The filtration system has the ability to remove 95–99% suspended solids and 90–99% of hydrocarbons originating from produced water, sea, surface and freshwater sources providing discharge levels of 5 ppm and lower. It is noteworthy that backwash process takes place using a specifically designed rotating media-scrubbing agitator rather than chemicals. Moreover, WS are utilized in the oil and gas industry as lost circulation material due to problems associated with drilling mud losses [126]. Due to the recent stringent environmental regulations, nutshell filters are the next generation technology. WS are used to remove oil and grease and suspended solids from a variety of chemical plants and oil fields with efficacy of 99% [127]. Very limited information is available online and as such, it is

Table 12
Kinetic models and their parameters for the adsorption of different contaminants on WS-based adsorbents.

Adsorbent	Contaminant	Pseudo first order			Pseudo second order			references
		q_e (mg/g)	K_1 (1/min)	R^2	q_e (mg/g)	K_2 (g/mg/min)	R^2	
Raw WS	Methylene blue dye	4.713	0.003	0.99	4.697	0.053	0.99	[98]
Raw WS	Alizarin yellow GG	3.9	0.051	0.79	4.5	0.0061	0.98	[107]
WS treated with acetic acid	Methylene blue dye	2	6.9×10^{-3}	0.86	6.5	8.72×10^{-3}	0.99	[42]
WS impregnated with Fe/Fe_3C nanoparticles	Methylene blue dye	11.3	0.06	0.69	529.1	0.02	1	[31]
Chemically modified by NaOH	Phosphorous	24.35	0.002	0.22	10.87	0.016	0.99	[22]
Chemically modified Levulinic acid WS	Methylene blue dye	2.983	0.015	0.73	99	0.017	0.99	[22]
Carboxylate-functionalized WS	Pb^{2+}	40.30	0.363	0.98	188.6	0.021	0.99	[85]
Arginine-doped polyaniline WS	Cr (VI)	152.8	0.118	0.92	163.3	11.1×10^{-4}	0.98	[81]
Diethylenetriamine modified WS	Cr (VI)	–	–	–	28.7	0.00266	0.96	[35]
WS modified with titanium dioxide	Humic acid	1.61	0.01	0.03	9.62	0.1	0.96	[117]
WS modified with zinc oxide	Humic acid	0.55	0.03	0.18	1.69	0.12	0.84	[86]
WS modified with aspartic acid	Reactive brilliant blue dye	106.8	0.05	0.72	113.4	0.582	0.99	[84]
Commercial activated WS	Naphthalene	42.12	0.081	0.98	105.2	0.00679	0.99	[84]
WS chemically activated with $ZnCL_2$	Dimethyl amino ethyl azide	97.05	0.116	0.85	181.8	0.0059	0.99	[39]
WS impregnated with $La(OH)_3$	Phosphate	17.81	0.267	0.95	19.82	0.0165	0.97	[34]
Amino modified WS	Pb^{2+}	74.26	0.044	0.66	54.35	0.002	0.99	[79]

difficult to provide more data on WS with regards to its industrial application. It is crucial that this information is available as it aids in solving current issues being faced in the industry and advancing current research works.

Several research works involving the preparation of WS-based adsorbents have been patented. Cao Jiashun invented a method for preparation of a cationic adsorbent from WS to be used in the adsorption of anionic dyes from wastewater originating from the printing and dye industry. This method involved the use of epoxychloropropane as the etherifying agent and diethylenetraiamine as the crosslinking agent. The process was carried out in an alkaline environment introducing the amino group in a two-step modification process [128]. It was reported that the resulting adsorbent has the ability to adsorb anionic azo dyes reaching a capacity of 500 mg/g which is 9 times the unmodified WS [128].Wang Dong invented a method to modify WS using KOH for the removal of methylene blue. [129]. The invention constituted of a simple process which involved the step of hydrothermally carbonizing WS after which it was mixed KOH solution. In the final step, KOH modified WS was placed in a tube furnace at a temperature of 800 °C for two hours [129]. Another WS-based adsorbent has been invented by Gao Jingfeng for the removal of methylene blue [130]. However, the method used is completely different from the one mentioned above. Prior to the carbonization process, WS were soaked in a 30% $ZnCl_2$ solution. As for the carbonization process, microwave irradiation technique has been utilized on 480–630 W [130]. The resulting adsorbent was washed with HCl until neutral conditions achieved.

10. Conclusions and future perspectives

In this review, the focus was on recent studies for the application of WS-based adsorbents for the removal of contaminants from water. WS have been employed for several industrial activities and more recently, in the water treatment industry. Due to their unique properties and naturally imbedded functional groups, they have been successfully employed for the removal organic compounds and heavy metal ions. According to the literature, WS have been used in four different methods, raw, chemically activated, physically activated and chemical modified or impregnated with different chemical compounds. Results indicated that Chemical activation stemmed morphological properties superior to all other modification processes. Resulting S_{BET} values reached 2000 m^2/g competing with commercially available AC. It has been noted that pyrolysis temperature should not exceed 500 to 600 °C as increasingly high temperatures will result in lower S_{BET} and total pore volumes.

Studies discussed in this review paper are mainly batch isotherm systems for evaluating the performance of different WS-based adsorbents. In addition to the morphological properties of the adsorbent, other entities that affect the mechanism of adsorption are the physicochemical properties and characteristics of target contaminants and the acidic/basic nature of the background solution chemistry. pH, temperature, and ionic strength are also key players in the adsorption process. Electrostatic interactions are the solely responsible for the adsorption of charged contaminants where altering pH changes surface chemistry inducing either repulsive or attractive forces between the adsorbent and adsorbate. In addition, the effect of pH greatly depends on the protonation/deprotonation of functional groups on the contaminant. Other mechanisms reported are Π-Π interactions and molecular configuration including size, aromaticity and functional groups are all viable contributors to the adsorption mechanism. Most studies reported the adsorption studies are endothermic in nature and spontaneous. Moreover, most systems followed the Freundlich isotherm model and the Pseudo-second order kinetic study. Structure of the AC can be altered according to target contaminant. For instance, creating a mesoporous structure will aid in contaminants with high molecular weight to navigate towards the adsorbent's micropores, thus, improving adsorption efficacy.

Essentially, laboratory data provided a valuable insight to the adsorption mechanisms onto WS-based adsorbents. Nonetheless, more studies are needed to be conducted on nonionic organic compounds in order to evaluate other adsorption mechanisms besides electrostatic interactions. Column-based and regeneration studies are limited and more tests should be conducted in both areas.

Declaration of Competing Interest

The authors declare that they have no known competing financial interests or personal relationships that could have appeared to influence the work reported in this paper.

Acknowledgment

HA wanted to acknowledge Qatar University for providing the Graduate assistantship.

Appendix A. Supplementary data

Supplementary data to this article can be found online at https://doi.org/10.1016/j.jwpe.2021.102527.

References

[1] Y. Chen, Y. Zhu, Z. Wang, Y. Li, L. Wang, L. Ding, X. Gao, Y. Ma, Y. Guo, Application studies of activated carbon derived from rice husks produced by chemical-thermal process—A review, Adv. Colloid Interf. Sci. 163 (2011) 39–52, https://doi.org/10.1016/J.CIS.2011.01.006.

[2] H. Albatrni, H. Qiblawey, M.H. El-Naas, Comparative study between adsorption and membrane technologies for the removal of mercury, Sep. Purif. Technol. 257 (2021), 117833, https://doi.org/10.1016/J.SEPPUR.2020.117833.

[3] Z. Chudhary, R.A. Khera, M.A. Hanif, M.A. Ayub, L. Hamrouni, Walnut, in: Medicinal Plants of South Asia, 2020, pp. 671–684, https://doi.org/10.1016/b978-0-08-102659-5.00049-5.

[4] C.S.G.P. Queirós, S. Cardoso, A. Lourenço, J. Ferreira, I. Miranda, M.J. V. Lourenço, H. Pereira, Characterization of walnut, almond, and pine nut shells regarding chemical composition and extract composition, Biomass Conversion Biorefinery. 10 (2020) 175–188, https://doi.org/10.1007/s13399-019-00424-2.

[5] J. Cañellas, A. Femenia, C. Rosselló, L. Soler, Chemical composition of the shell of apricot seeds, J. Sci. Food Agric. (1992), https://doi.org/10.1002/jsfa.2740590220.

[6] M.L. Martínez, L. Moiraghi, M. Agnese, C. Guzman, Making and some properties of activated carbon produced from agricultural industrial residues from aargentina, Anales Des La Asociacion Quimica Argentina. 91 (4) (2003) 103–108.

[7] H. Pirayesh, A. Khazaeian, T. Tabarsa, The potential for using walnut (Juglans regia L.) shell as a raw material for wood-based particleboard manufacturing, Compos. Part B 43 (2012) 3276–3280, https://doi.org/10.1016/j.compositesb.2012.02.016.

[8] E. Schröder, K. Thomauske, C. Weber, A. Hornung, V. Tumiatti, Experiments on the generation of activated carbon from biomass, J. Anal. Appl. Pyrolysis 79 (2007) 106–111, https://doi.org/10.1016/j.jaap.2006.10.015.

[9] L.T. Popoola, Tetracycline and sulfamethoxazole adsorption onto nanomagnetic walnut shell-rice husk: isotherm, kinetic, mechanistic and thermodynamic studies, Int. J. Environ. Anal. Chem. 100 (2020) 1021–1043, https://doi.org/10.1080/03067319.2019.1646739.

[10] C. Kang, L. Zhu, Y. Wang, Y. Wang, K. Xiao, T. Tian, Adsorption of basic dyes using walnut Shell-based biochar produced by hydrothermal carbonization, Chem. Res. Chin. Univ. 34 (2018) 622–627, https://doi.org/10.1007/s40242-018-8018-0.

[11] A. Morales, J. Labidi, P. Gullón, Hydrothermal treatments of walnut shells: a potential pretreatment for subsequent product obtaining, Sci. Total Environ. 764 (2020), 142800, https://doi.org/10.1016/j.scitotenv.2020.142800.

[12] G. Nazari, H. Abolghasemi, M. Esmaieli, Batch adsorption of cephalexin antibiotic from aqueous solution by walnut shell-based activated carbon, J. Taiwan Inst. Chem. Eng. 58 (2016) 357–365, https://doi.org/10.1016/j.jtice.2015.06.006.

[13] G. Nazari, H. Abolghasemi, M. Esmaieli, M. Assar, Theoretical and experimental study of cephalexin batch adsorption dynamics using walnut shell-based activated carbon, Desalin. Water Treat. 57 (2016) 27339–27348, https://doi.org/10.1080/19443994.2016.1172029.

[14] A. Srinivasan, T. Viraraghavan, Removal of oil by walnut shell media, Bioresour. Technol. 99 (2008) 8217–8220, https://doi.org/10.1016/j.biortech.2008.03.072.

[15] K. Kuśmierek, A. Świątkowski, L. Dąbek, Removal of 2, 4, 6-trichlorophenol from aqueous solutions using agricultural waste as low-cost adsorbents, Environ. Prot. Eng. (2017), https://doi.org/10.5277/epel70412.

[16] M. Zhu, J. Yao, L. Dong, J. Sun, Adsorption of naphthalene from aqueous solution onto fatty acid modified walnut shells, Chemosphere 144 (2016) 1639–1645, https://doi.org/10.1016/j.chemosphere.2015.10.050.

[17] Q. Yu, M. Li, X. Ji, Y. Qiu, Y. Zhu, C. Leng, Characterization and methanol adsorption of walnut-shell activated carbon prepared by KOH activation, J. Wuhan Univ. Technol. Mater. Sci. Ed. 31 (2016) 260–268, https://doi.org/10.1007/s11595-016-1362-3.

[18] M. Dias, J. Pinto, B. Henriques, P. Figueira, E. Fabre, D. Tavares, C. Vale, E. Pereira, Nutshells as efficient biosorbents to remove cadmium, lead, and mercury from contaminated solutions, Int. J. Environ. Res. Publ. Health 18 (2021) 1–17, https://doi.org/10.3390/ijerph18041580.

[19] X. Yin, J. Zhang, X. Wang, M. Zhu, Modified walnut shell filter material for the enhanced removal of oil from oilfield wastewater, Environ. Eng. Res. 26 (2021) 1–6, https://doi.org/10.4491/eer.2019.369.

[20] A. Demirbas, Effect of temperature on pyrolysis products from four nut shells, J. Anal. Appl. Pyrolysis 76 (2006) 285–289, https://doi.org/10.1016/j.jaap.2005.12.012.

[21] S. Román, J.M.V. Nabais, B. Ledesma, C. Laginhas, M.M. Titirici, Surface interactions during the removal of emerging contaminants by hydrochar-based adsorbents, Molecules 25 (2020) 1–12, https://doi.org/10.3390/molecules25092264.

[22] S. Teixeira, C. Delerue-Matos, L. Santos, Application of experimental design methodology to optimize antibiotics removal by walnut shell based activated carbon, Sci. Total Environ. 646 (2019) 168–176, https://doi.org/10.1016/j.scitotenv.2018.07.204.

[23] P.L. de Hoyos-Martínez, X. Erdocia, F. Charrier-El Bouhtoury, R. Prado, J. Labidi, Multistage treatment of almonds waste biomass: characterization and assessment of the potential applications of raw material and products, Waste Manag. (2018), https://doi.org/10.1016/j.wasman.2018.08.051.

[24] A. Jahanban-Esfahlan, R. Amarowicz, Walnut (: Juglans regia L.) shell pyroligneous acid: chemical constituents and functional applications, RSC Adv. 8 (2018) 22376–22391, https://doi.org/10.1039/c8ra03684e.

[25] A. Jahanban-Esfahlan, A. Ostadrahimi, M. Tabibiazar, R. Amarowicz, A comprehensive review on the chemical constituents and functional uses of walnut (Juglans spp.) husk, Int. J. Mol. Sci. 20 (2019), https://doi.org/10.3390/ijms20163920.

[26] M. Zhai, G. Shi, Y. Wang, G. Mao, D. Wang, Z. Wang, Chemical compositions and biological activities of pyroligneous acids from walnut shell, Bioresources 10 (2015) 1715–1729, https://doi.org/10.15376/biores.10.1.1715-1729.

[27] E.V. Mathias, U.P. Halkar, Separation and characterization of lignin compounds from the walnut (Juglans regia) shell oil using preparative TLC, GC-MS and 1H NMR, J. Anal. Appl. Pyrolysis. 71 (2004) 515–524, https://doi.org/10.1016/j.jaap.2003.08.005.

[28] M.F. de Lange, T.J.H. Vlugt, J. Gascon, F. Kapteijn, Adsorptive characterization of porous solids: error analysis guides the way, Microporous Mesoporous Mater. 200 (2014) 199–215, https://doi.org/10.1016/j.micromeso.2014.08.048.

[29] M. Ashrafi, G. Bagherian, M.A. Chamjangali, N. Goudarzi, Removal of Brilliant green and crystal violet from mono- and Bi-component aqueous solutions using NaOH-modified walnut shell, Anal. Bioanal.Chem. Res. 5 (2018) 95–114, https://doi.org/10.22036/abcr.2018.106139.1172.

[30] M. Bayat, A. Alighardashi, A. Sadeghasadi, Fixed-bed column and batch reactors performance in removal of diazinon pesticide from aqueous solutions by using walnut shell-modified activated carbon, Environ. Technol. Innov. 12 (2018) 148–159, https://doi.org/10.1016/j.eti.2018.08.008.

[31] J. Zhou, C. Zhang, T. Niu, R. Huang, S. Li, J. Sun, Y. Wang, Facile synthesis of reusable magnetic Fe/Fe3C/C composites from renewable resources for super-fast removal of organic dyes: characterization, mechanism and kinetics, Powder Technol. 351 (2019) 314–324, https://doi.org/10.1016/j.powtec.2019.04.016.

[32] P. Liu, Z. Wu, Z. Sun, J. Ye, Comparison study of naphthalene adsorption on activated carbons prepared from different raws, Korean J. Chem. Eng. 35 (2018) 2086–2096, https://doi.org/10.1007/s11814-018-0124-7.

[33] A. Alkhouzaam, H. Qiblawey, M. Khraisheh, M. Atieh, M. Al-Ghouti, Synthesis of graphene oxides particle of high oxidation degree using a modified hummers method, Ceram. Int. 46 (2020) 23997–24007, https://doi.org/10.1016/j.ceramint.2020.06.177.

[34] Y. Luo, K. Xie, Y. Feng, Q. He, K. Zhang, S. Shen, Synthesis of a La (OH) 3 nanorod / walnut shell biochar composite for reclaiming phosphate from aqueous solutions, Coll. Surf. A : Physicochem. Eng. Aspects Syn. (2020) 1–12.

[35] M. Ashrafi, H. Borzuie, G. Bagherian, M.A. Chamjangali, H. Nikoofard, Artificial neural network and multiple linear regression for modeling sorption of Pb2+ ions from aqueous solutions onto modified walnut shell, Separat. Sci. Technol. (Philadelphia). 55 (2020) 222–233, https://doi.org/10.1080/01496395.2019.1577437.

[36] S. Hajialigol, S. Masoum, Optimization of biosorption potential of nano biomass derived from walnut shell for the removal of Malachite Green from liquids solution: experimental design approaches, J. Mol. Liq. 286 (2019), 110904, https://doi.org/10.1016/j.molliq.2019.110904.

[37] P. Ning, S. Liu, C. Wang, K. Li, X. Sun, L. Tang, G. Liu, Adsorption-oxidation of hydrogen sulfide on Fe/walnut-shell activated carbon surface modified by NH3-plasma, J. Environ. Sci. (China) 64 (2018) 216–226, https://doi.org/10.1016/j.jes.2017.06.017.

[38] Y. Yu, Q. An, Y. Zhou, S. Deng, Y. Miao, B. Zhao, L. Yang, Highly synergistic effects on ammonium removal by the co-system of pseudomonas stutzeri XL-2 and modified walnut shell biochar, Bioresour. Technol. 280 (2019) 239–246, https://doi.org/10.1016/j.biortech.2019.02.037.

[39] S. Li, Z. Zeng, W. Xue, Kinetic and equilibrium study of the removal of reactive dye using modified walnut shell, Water Sci. Technol. 80 (2019) 874–883, https://doi.org/10.2166/wst.2019.324.

[40] X. Zheng, H. Lin, Y. Tao, H. Zhang, Selective adsorption of phenanthrene dissolved in tween 80 solution using activated carbon derived from walnut shells, Chemosphere 208 (2018) 951–959, https://doi.org/10.1016/j.chemosphere.2018.06.025.

[41] L. Wu, Z. Shang, S. Chen, J. Tu, N. Kobayashi, Z. Li, Raw walnut shell modified by non-thermal plasma in ultrafine water mist for adsorptive removal of Cu(ii) from aqueous solution, RSC Adv. 8 (2018) 21993–22003, https://doi.org/10.1039/c8ra03271h.

[42] V. Halysh, O. Sevastyanova, A.V. Riazanova, B. Pasalskiy, T. Budnyak, M. E. Lindström, M. Kartel, Walnut shells as a potential low-cost lignocellulosic sorbent for dyes and metal ions, Cellulose. 25 (2018) 4729–4742, https://doi.org/10.1007/s10570-018-1896-y.

[43] M. Liu, X. Li, Y. Du, R. Han, Adsorption of methyl blue from solution using walnut shell and reuse in a secondary adsorption for Congo red, Bioresource Technol. Rep. 5 (2019) 238–242, https://doi.org/10.1016/j.biteb.2018.11.006.

[44] M. Banerjee, R.K. Basu, S.K. Das, Cr(VI) adsorption by a green adsorbent walnut shell: adsorption studies, regeneration studies, scale-up design and economic feasibility, Process Saf. Environ. Prot. 116 (2018) 693–702, https://doi.org/10.1016/j.psep.2018.03.037.

[45] L.T. Popoola, Nano-magnetic walnut shell-rice husk for Cd(II) sorption: design and optimization using artificial intelligence and design expert, Heliyon. 5 (2019), e02381, https://doi.org/10.1016/j.heliyon.2019.e02381.

[46] Q. Shao, Y. Li, Q. Wang, T. Niu, S. Li, W. Shen, Preparation of copper doped walnut shell-based biochar for efficiently removal of organic dyes from aqueous solutions, J. Mol. Liq. 336 (2021), 116314, https://doi.org/10.1016/j.molliq.2021.116314.

[47] F. Rodríguez-Reinoso, M. Molina-Sabio, Activated carbons from lignocellulosic materials by chemical and/or physical activation: an overview, Carbon 30 (1992) 1111–1118, https://doi.org/10.1016/0008-6223(92)90143-K.

[48] C. Bouchelta, M.S. Medjram, O. Bertrand, J.P. Bellat, Preparation and characterization of activated carbon from date stones by physical activation with steam, J. Anal. Appl. Pyrolysis 82 (2008) 70–77, https://doi.org/10.1016/j.jaap.2007.12.009.
[49] O. Ioannidou, A. Zabaniotou, Agricultural residues as precursors for activated carbon production-a review, Renew. Sust. Energ. Rev. 11 (2007) 1966–2005, https://doi.org/10.1016/j.rser.2006.03.013.
[50] M.A. Yahya, Z. Al-Qodah, C.W.Z. Ngah, Agricultural bio-waste materials as potential sustainable precursors used for activated carbon production: a review, Renew. Sust. Energ. Rev. 46 (2015) 218–235, https://doi.org/10.1016/j.rser.2015.02.051.
[51] M. Pazouki, M. Zabihi, J. Shayegan, M.H. Fatehi, Mercury ion adsorption on AC@Fe3O4-NH2-COOH from saline solutions: experimental studies and artificial neural network modeling, Korean J. Chem. Eng. 35 (2018) 671–683, https://doi.org/10.1007/s11814-017-0293-9.
[52] K. Derdour, C. Bouchelta, A.K. Naser-Eddine, M.S. Medjram, P. Magri, Removal of Cr(VI) from aqueous solutions by using activated carbon supported iron catalysts as efficient adsorbents, WorldJ. Eng. 15 (2018) 3–13, https://doi.org/10.1108/WJE-06-2017-0132.
[53] Z. Heidarinejad, M.H. Dehghani, M. Heidari, G. Javedan, I. Ali, M. Sillanpää, Methods for preparation and activation of activated carbon: a review, Environ. Chem. Lett. 18 (2020) 393–415, https://doi.org/10.1007/s10311-019-00955-0.
[54] A. Ahmadpour, D.D. Do, The preparation of activated carbon from macadamia nutshell by chemical activation, Carbon (1997), https://doi.org/10.1016/S0008-6223(97)00127-9.
[55] X.Y. Cui, F. Jia, Y.X. Chen, J. Gan, Influence of single-walled carbon nanotubes on microbial availability of phenanthrene in sediment, Ecotoxicology (2011), https://doi.org/10.1007/s10646-011-0684-3.
[56] M.K.B. Gratuito, T. Panyathanmaporn, R.A. Chumnanklang, N. Sirinuntawittaya, A. Dutta, Production of activated carbon from coconut shell: optimization using response surface methodology, Bioresour. Technol. (2008), https://doi.org/10.1016/j.biortech.2007.09.042.
[57] Z. Alimohammadi, H. Younesi, Batch and column adsorption of reactive red 198 from textile industry effluent by microporous activated carbon developed from walnut shells, Waste Biomass Valorizat. 7 (2016) 1255–1270, https://doi.org/10.1007/s12649-016-9506-4.
[58] T.A. Ojo, A.T. Ojedokun, O.S. Bello, Functionalization of powdered walnut shell with orthophosphoric acid for Congo red dye removal, Part. Sci. Technol. 37 (2019) 74–85, https://doi.org/10.1080/02726351.2017.1340914.
[59] A. Alighardashi, S. Shahali, Removal of nitrate from synthetic aqueous solution and groundwater in a continuous pilot system using chemical activated carbon derived from walnut shell, Water Practice Technol. 11 (2016) 784–795, https://doi.org/10.2166/wpt.2016.082.
[60] G. Wang, L. He, M. Wang, S. Tang, Y. Chen, Enhancing removal of Cu(II) from aqueous solution by walnut shell-based activated carbon with pyrolusite modification, Int. J. Environ. Anal. Chem. 00 (2020) 1–13, https://doi.org/10.1080/03067319.2020.1814268.
[61] J. Donald, Y. Ohtsuka, C.C. Xu, Effects of activation agents and intrinsic minerals on pore development in activated carbons derived from a Canadian peat, Mater. Lett. 65 (2011) 744–747, https://doi.org/10.1016/j.matlet.2010.11.049.
[62] Z. Wu, Z. Sun, P. Liu, Q. Li, R. Yang, X. Yang, Competitive adsorption of naphthalene and phenanthrene on walnut shell based activated carbon and the verification: via theoretical calculation, RSC Adv. 10 (2020) 10703–10714, https://doi.org/10.1039/c9ra09447d.
[63] J. Zhang, L. Fu, J. Gao, Y. Chen, X. Hao, Ordered mesoporous TiO 2 /Activated carbon for adsorption and photocatalysis of acid red 18, Solution 12 (2017) 9086–9102.
[64] V.O. Njoku, K.Y. Foo, B.H. Hameed, Microwave-assisted preparation of pumpkin seed hull activated carbon and its application for the adsorptive removal of 2,4-dichlorophenoxyacetic acid, Chem. Eng. J. 215–216 (2013) 383–388, https://doi.org/10.1016/j.cej.2012.10.068.
[65] M.J. Ahmed, S.K. Theydan, Optimization of microwave preparation conditions for activated carbon from Albizia lebbeck seed pods for methylene blue dye adsorption, J. Anal. Appl. Pyrolysis 105 (2014) 199–208, https://doi.org/10.1016/j.jaap.2013.11.005.
[66] A. Bhatnagar, W. Hogland, M. Marques, M. Sillanpää, An overview of the modification methods of activated carbon for its water treatment applications, Chem. Eng. J. 219 (2013) 499–511, https://doi.org/10.1016/j.cej.2012.12.038.
[67] Q. Shao, Y. Li, Q. Wang, T. Niu, S. Li, W. Shen, Preparation of copper doped walnut shell-based biochar for efficiently removal of organic dyes from aqueous solutions, J. Mol. Liq. 336 (2021), https://doi.org/10.1016/j.molliq.2021.116314.
[68] Z.A. Alothman, M.A. Habila, R. Ali, Preparation of activated carbon using the copyrolysis of agricultural and municipal solid wastes at a low carbonization temperature, in: Proceedings of the International Conference on Biological and Envrinemntal Chemistry, 2011, pp. 67–72, https://doi.org/10.13140/2.1.1478.2401.
[69] A. Akbarzadeh, M. Arbabi, S. Hemati, Preparation of controlled porosity activated carbon from walnut shell for phenol adsorption, Desalin. Water Treat. 130 (2018) 63–70, https://doi.org/10.5004/dwt.2018.22642.
[70] Z. Teimouri, A. Salem, S. Salem, Microwave-assisted for clean and rapid fabrication of highly efficient magnetically separable activated carbon from agriculture shells for low grade industrial corn syrup decoloration: a novel strategy for impregnation of ternary catalytic composite, Food Bioprod. Process. 116 (2019) 78–88, https://doi.org/10.1016/j.fbp.2019.04.013.
[71] S.G. Pakdehi, F. Rezaei, Adsorption of liquid fuel dimethyl amino ethyl azide from dilute aqueous solution on activated carbon prepared from walnut shell 3994, 2016, https://doi.org/10.1080/19443994.2016.1175969.
[72] Z. Li, H. Hanafy, L. Zhang, L. Sellaoui, M. Schadeck Netto, M.L.S. Oliveira, M. K. Seliem, G. Luiz Dotto, A. Bonilla-Petriciolet, Q. Li, Adsorption of Congo red and methylene blue dyes on an ashitaba waste and a walnut shell-based activated carbon from aqueous solutions: experiments, characterization and physical interpretations, Chem. Eng. J. 388 (2020), 124263, https://doi.org/10.1016/j.cej.2020.124263.
[73] A.Y. Wang, K. Sun, L. Wu, P. Wu, W. Zeng, Z. Tian, Q.X. Huang, Co-carbonization of biomass and oily sludge to prepare sulfamethoxazole super-adsorbent materials, Sci. Total Environ. 698 (2020), 134238, https://doi.org/10.1016/j.scitotenv.2019.134238.
[74] D. Adinata, W.M.A. Wan Daud, M.K. Aroua, Preparation and characterization of activated carbon from palm shell by chemical activation with K2CO3, Bioresour. Technol. 98 (2007) 145–149, https://doi.org/10.1016/j.biortech.2005.11.006.
[75] D. Özçimen, A. Ay, segül Ersoy-Meriçboyu, Adsorption of Copper(II) Ions onto Hazelnut Shell and Apricot Stone Activated Carbons, 2021.
[76] Z. Xu, Y. Zhou, Z. Sun, D. Zhang, Y. Huang, S. Gu, W. Chen, Understanding reactions and pore-forming mechanisms between waste cotton woven and FeCl3 during the synthesis of magnetic activated carbon, Chemosphere (2020), https://doi.org/10.1016/j.chemosphere.2019.125120.
[77] J. Bedia, M. Peñas-Garzón, A. Gómez-Avilés, J.J. Rodriguez, C. Belver, Review on activated carbons by chemical activation with FeCl3, C — J. CarbonRes. (2020), https://doi.org/10.3390/c6020021.
[78] P. Nowicki, R. Pietrzak, H. Wachowska, Sorption properties of active carbons obtained from walnut shells by chemical and physical activation, Catal. Today 150 (2010) 107–114, https://doi.org/10.1016/j.cattod.2009.11.009.
[79] G. Liu, W. Zhang, R. Luo, Synthesis, characterization of amino - modified walnut shell, Polym. Bull. 76 (2019) 1099–1114, https://doi.org/10.1007/s00289-018-2424-9.
[80] J.S. Cao, J.X. Lin, F. Fang, M.T. Zhang, Z.R. Hu, A new absorbent by modifying walnut shell for the removal of anionic dye: kinetic and thermodynamic studies, Bioresour. Technol. 163 (2014) 199–205, https://doi.org/10.1016/j.biortech.2014.04.046.
[81] S. Kocaman, Removal of methylene blue dye from aqueous solutions by adsorption on levulinic acid-modified natural shells, Int. J. Phytoremed. 22 (2020) 885–895, https://doi.org/10.1080/15226514.2020.1736512.
[82] D. Xu, W.D. Wu, H.J. Qi, R.X. Yang, W.Q. Deng, Sulfur rich microporous polymer enables rapid and efficient removal of mercury(II) from water, Chemosphere 196 (2018) 174–181, https://doi.org/10.1016/j.chemosphere.2017.12.186.
[83] S. Li, M. Qiu, Z. Zeng, W. Xue, Effective modified walnut Shell adsorbent: synthesis and adsorption behavior for Pb2+ and Ni2+ from aqueous solution, Environ. Eng. Sci. 36 (2019) 1421–1432, https://doi.org/10.1089/ees.2019.0227.
[84] I.W.A. Publishing, in: Synthesis of walnut shell modified with titanium dioxide and zinc oxide nanoparticles for ef fi cient removal of humic acid from aqueous solutions Ali Naghizadeh , Habibeh Shahabi , Fatemeh Ghasemi and Ahmad Zarei, 2016, pp. 989–997, https://doi.org/10.2166/wh.2016.072.
[85] B. Faraji, M. Zarabi, Z. Kolahchi, Phosphorus removal from aqueous solution using modified walnut and almond wooden shell and recycling as soil amendment, Environ. Monit. Assess. 192 (2020), https://doi.org/10.1007/s10661-020-08326-x.
[86] J. Li, J. Ma, Q. Guo, S. Zhang, H. Han, S. Zhang, R. Han, Adsorption of hexavalent chromium using modified walnut shell from solution, Water Sci. Technol. 81 (2020) 824–833, https://doi.org/10.2166/wst.2020.165.
[87] A. Imgharn, H. Ighnih, A. Hsini, Y. Naciri, M. Laabd, H. Kabli, M. Elamine, R. Lakhmiri, B. Souhail, A. Albourine, Synthesis and characterization of polyaniline-based biocomposites and their application for effective removal of Orange G dye using adsorption in dynamic regime, Chem. Phys. Lett. 778 (2021), 138811, https://doi.org/10.1016/j.cplett.2021.138811.
[88] X.G. Lu, Y.T. Guo, Removal of pb (II) from aqueous solution by sulfur-functionalized walnut shell, Environ. Sci. Pollut. Res. 26 (2019) 12776–12787, https://doi.org/10.1007/s11356-019-04753-7.
[89] P. Hadi, M.H. To, C.W. Hui, C.S.K. Lin, G. McKay, Aqueous mercury adsorption by activated carbons, Water Res. 73 (2015) 37–55, https://doi.org/10.1016/j.watres.2015.01.018.
[90] R. Tang, C. Dai, C. Li, W. Liu, S. Gao, C. Wang, Removal of methylene blue from aqueous solution using agricultural residue walnut Shell: equilibrium, kinetic, and thermodynamic studies, J. Chem. 2017 (2017), https://doi.org/10.1155/2017/8404965.
[91] A. Gallo-Cordova, M.D.M. Silva-Gordillo, G.A. Muñoz, X. Arboleda-Faini, D. Almeida Streitwieser, Comparison of the adsorption capacity of organic compounds present in produced water with commercially obtained walnut shell and residual biomass, J. Environ. Chem. Eng. 5 (2017) 4041–4050, https://doi.org/10.1016/j.jece.2017.07.052.
[92] Y. Miyah, A. Lahrichi, M. Idrissi, A. Khalil, F. Zerrouq, Adsorption of methylene blue dye from aqueous solutions onto walnut shells powder: equilibrium and kinetic studies, Surf. Interfaces. 11 (2018) 74–81, https://doi.org/10.1016/j.surfin.2018.03.006.
[93] J. Li, Z. Zhao, D. Li, X. Tang, H. Feng, W. Qi, Q. Wang, Multifunctional walnut shell layer used for oil/water mixtures separation and dyes adsorption, Appl. Surf. Sci. 419 (2017) 869–874, https://doi.org/10.1016/j.apsusc.2017.05.114.
[94] H. Çelebi, O. Gök, Evaluation of Lead adsorption kinetics and isotherms from aqueous solution using natural walnut shell, Int.J. Environ. Res. 11 (2017) 83–90, https://doi.org/10.1007/s41742-017-0009-3.

[95] K. Kusmierek, A. Swiatkowski, L. Dabek, Removal 2,4,6-trichlorophenol of from aqueous solutions using agricultural waste as low-cost adsorbents, Environ. Prot. Eng. 43 (2017) 149–163, https://doi.org/10.5277/epe170412.
[96] Y. Song, H. Fang, H. Xu, X. Tan, S. Chen, Treatment of wastewater containing crystal violet using walnut shell, J. Residuals Sci. Technol. 13 (2016) 243–249, https://doi.org/10.12783/issn.1544-8053/13/4/1.
[97] R. Najam, S.M.A. Andrabi, Removal of Cu(II), Zn(II) and Cd(II) ions from aqueous solutions by adsorption on walnut shell-equilibrium and thermodynamic studies: treatment of effluents from electroplating industry, Desalin. Water Treat. 57 (2016) 27363–27373, https://doi.org/10.1080/19443994.2016.1166350.
[98] M.K. Uddin, A. Nasar, Walnut shell powder as a low-cost adsorbent for methylene blue dye: isotherm, kinetics, thermodynamic, desorption and response surface methodology examinations, Sci. Rep. 10 (2020) 1–13, https://doi.org/10.1038/s41598-020-64745-3.
[99] B. Karbowska, E. Konował, W. Zembrzuski, G. Milczarek, Sorption of thallium on walnut shells and its enhancement by the lignosulfonate-stabilized gold colloid, Pol. J. Environ. Stud. 28 (2019) 2151–2158, https://doi.org/10.15244/pjoes/86217.
[100] T. Bakalar, H. Pavolova, Application of organic waste for adsorption of zn(II) and cd(II) ions, Environ. Prot. Eng. 45 (2019) 35–54, https://doi.org/10.5277/epe190203.
[101] S. Davidi, A. Lashanizadegan, H. Sharififard, Walnut shell activated carbon: optimization of synthesis process, characterization and application for zn (II) removal in batch and continuous process, Mater.Res. Express. 6 (2019), https://doi.org/10.1088/2053-1591/ab213e.
[102] Y. Miyah, A. Lahrichi, R. Kachkoul, G. el Mouhri, M. Idrissi, S. Iaich, F. Zerrouq, Multi-parametric filtration effect of the dyes mixture removal with the low cost materials, Arab J. Basic Appl. Sci 27 (2020) 248–258, https://doi.org/10.1080/25765299.2020.1776008.
[103] E. Loffredo, Y. Scarcia, M. Parlavecchia, Removal of ochratoxin A from liquid media using novel low-cost biosorbents, Environ. Sci. Pollut. Res. 27 (2020) 34484–34494, https://doi.org/10.1007/s11356-020-09544-z.
[104] Ç. Sarici Özdemİr, Adsorptive removal of methylene blue by fruit shell: isotherm studies, Fullerenes Nanotubes Carbon Nanostruct 26 (2018) 570–577, https://doi.org/10.1080/1536383X.2018.1472083.
[105] L. Zhang, X. Li, Y. Huang, Y. Ma, X. Wan, Y. Chen, Controlled synthesis of few-layered graphene sheets on a large scale using chemical exfoliation, Carbon 48 (2010) 2367–2371, https://doi.org/10.1016/j.carbon.2010.02.035.
[106] L.Hua Jiang, Y.Guo Liu, G.Ming Zeng, F.Yu Xiao, X.Jiang Hu, X. Hu, H. Wang, T. Ting Li, L. Zhou, X.Fei Tan, Removal of 17β-estradiol by few-layered graphene oxide nanosheets from aqueous solutions: External influence and adsorption mechanism, Chem. Eng. J. 284 (2016) 93–102, https://doi.org/10.1016/j.cej.2015.08.139.
[107] N. Kaya, Z.Y. Uzun, Investigation of effectiveness of pyrolysis products on removal of alizarin yellow GG from aqueous solution: a comparative study with commercial activated carbon, Water Sci. Technol. 81 (2020) 1191–1208, https://doi.org/10.2166/wst.2020.213.
[108] Q. Yu, M. Li, P. Ning, H. Yi, X. Tang, Characterization of metal oxide-modified walnut-shell activated carbon and its application for phosphine adsorption: equilibrium, regeneration, and mechanism studies, J. Wuhan Univ. Technol. Mater. Sci. Ed. 34 (2019) 487–495, https://doi.org/10.1007/s11595-019-2078-y.
[109] E.G. Lemraski, S. Sharafinia, Kinetics, equilibrium and thermodynamics studies of Pb2+ adsorption onto new activated carbon prepared from Persian mesquite grain, J. Mol. Liq. 219 (2016) 482–492, https://doi.org/10.1016/j.molliq.2016.03.031.
[110] H. Albatrni, H. Qiblawey, F. Almomani, S. Adham, M. Khraisheh, Polymeric adsorbents for oil removal from water, Chemosphere 233 (2019) 809–817, https://doi.org/10.1016/j.chemosphere.2019.05.263.
[111] G. Limousin, J.P. Gaudet, L. Charlet, S. Szenknect, V. Barthès, M. Krimissa, Sorption isotherms: a review on physical bases, modeling and measurement, Appl. Geochem. 22 (2007) 249–275, https://doi.org/10.1016/j.apgeochem.2006.09.010.
[112] R. Yousef, H. Qiblawey, M.H. El-Naas, Adsorption as a process for produced water treatment: a review, Processes. 8 (2020) 1–22, https://doi.org/10.3390/pr8121657.
[113] I. Langmuir, The adsorption of gases on plane surfaces of glassmica and platinum, J. Am. Chem. Soc. 40 (1918) 1361–1403.
[114] S. Ayoob, A.K. Gupta, Insights into isotherm making in the sorptive removal of fluoride from drinking water, J. Hazard. Mater. 152 (2008) 976–985, https://doi.org/10.1016/j.jhazmat.2007.07.072.
[115] S.J. Allen, G. Mckay, J.F. Porter, Adsorption isotherm models for basic dye adsorption by peat in single and binary component systems, J. Colloid Interface Sci. 280 (2004) 322–333, https://doi.org/10.1016/j.jcis.2004.08.078.
[116] Y.S. Ho, J.F. Porter, G. McKay, Equilibrium isotherm studies for the sorption of divalent metal ions onto peat: copper, nickel and lead single component systems, Water Air Soil Pollut. 141 (2002) 1–33, https://doi.org/10.1023/A:1021304828010.
[117] A. Hsini, Y. Naciri, M. Laabd, M. el Ouardi, Z. Ajmal, R. Lakhmiri, R. Boukherroub, A. Albourine, Synthesis and characterization of arginine-doped polyaniline/walnut shell hybrid composite with superior clean-up ability for chromium (VI) from aqueous media: equilibrium, reusability and process optimization, J. Mol. Liq. 316 (2020), 113832, https://doi.org/10.1016/j.molliq.2020.113832.
[118] N.S. Beyranvand, B. Samiey, A.D. Tehrani, Adsorption mechanism of Congo red on Mg–Al-layered double hydroxide nanocompound, Acta Chim. Slov. 66 (2019) 443–454, https://doi.org/10.17344/acsi.2018.4920.
[119] M. Rafi, B. Samiey, C.H. Cheng, Study of adsorption mechanism of Congo red on graphene oxide/PAMAM nanocomposite, Materials. 11 (2018) 1–24, https://doi.org/10.3390/ma11040496.
[120] K.L. Tan, B.H. Hameed, Insight into the adsorption kinetics models for the removal of contaminants from aqueous solutions, J. Taiwan Inst. Chem. Eng. 74 (2017) 25–48, https://doi.org/10.1016/j.jtice.2017.01.024.
[121] D. Ewis, A. Benamor, M.M. Ba-Abbad, M. Nasser, M. El-Naas, H. Qiblawey, Removal of oil content from oil-water emulsions using iron Oxide/Bentonite Nano adsorbents, J. Water Process Eng. 38 (2020), https://doi.org/10.1016/j.jwpe.2020.101583.
[122] I. Lagergren, About the theory of so-called adsorption of soluble substances, K. Sven. Vetenskapsakad. Handl. 24 (1898) 1–39.
[123] G. Mckay, Y.S. Ho, J.C.Y. Ng, Biosorption of copper from waste waters: a review, separation and purification methods, Separat. Purif. Methods. 28 (1999) 87–125, https://doi.org/10.1080/03602549909351645.
[124] Y.S. Ho, G. McKay, Pseudo-second order model for sorption processes, Process Biochem. 34 (1999) 451–465, https://doi.org/10.1016/S0032-9592(98)00112-5.
[125] Schlumberger, PETRECO HYDROMATION Nutshell Filter, 2016.
[126] Eco-Shell, Industries and applications of walnut shell, 2021.
[127] Eco-Shell, Industries and applications of walnut shell, 2017.
[128] C. Jiashun, L. Junxiong, F. Fang, Z. Mingting, J. Xin, S. Qiao, J. Hui, Preparation method for modified walnut shell cation adsorbent, CN103381357A, 2013.
[129] W. Dong, Z. Hao, Y. Dongmei, Y. Jona, Method for preparing KOH-based modified walnut shell biomass hydrothermal carbonCN106000298A, 2016.
[130] G. Jingfeng, S. Chunying, Y. Chen, Method for removing methylene blue dye in wastewater through walnut shell biomass charcoal adsorbent CN103848473A, 2014.